

1 **Resolving the transcriptional transitions associated with**
2 **oligodendrocyte generation from adult neural stem cells by**
3 **single cell sequencing**

4 **Running Title: Oligodendroglial transcriptional networks**
5
6

7 Kasum Azim^{1*}, Filippo Calzolari², Martina Cantone³, Rainer Akkermann¹, Julio Vera⁴,
8 Hans-Peter Hartung¹, Onur Basak⁵, Arthur Morgan Butt⁶, Patrick Küry^{1*}

9 ¹ Department of Neurology, Medical Faculty, Heinrich-Heine-University, 40225
10 Düsseldorf, Germany.

11 ² Institute for Physiological Chemistry, University Medical Centre of the Johannes
12 Gutenberg University Mainz, Mainz, Germany.

13 ³ Faculty of Mechanical Engineering, Specialty Division for Systems Biotechnology,
14 Technische Universität München, Germany.

15 ⁴ Laboratory of Systems Tumor Immunology, Department of Dermatology, Friedrich-
16 Alexander-Universität Erlangen-Nürnberg, Erlangen, Germany.

17 ⁵ Department of Translational Neuroscience, UMC Utrecht Brain Centre, University
18 Medical Centre Utrecht, Utrecht University, Utrecht, The Netherlands.

19 ⁶ Institute of Biomedical and Biomolecular Sciences, School of Pharmacy and
20 Biomedical Science, University of Portsmouth, St Michael's Building, White Swan
21 Road, Portsmouth, PO1 2DT, UK.

22 * Corresponding Authors

23 Email: Kasum.Azim@med.uni-duesseldorf.de; kuqry@uni-duesseldorf.de.

24

25 **ACKNOWLEDGEMENTS**

26 We wish to thank Dominic Grün at the Max Planck Institute of Immunobiology and
27 Epigenetics in Freiburg, DE for his valuable expertise with the pseudotime analysis.

28 We also wish to thank Dr Marco Antonio Mendoza at Genoscope, FR, for
29 establishment, guidance and optimization of TETRAMER.

30

31 **Word count: 13,928 (inc References and Figure Legends)**

32

33 **Abstract**

34 The subventricular zone (SVZ) is the largest neurogenic niche in the adult forebrain.
35 Notably, neural stem cells (NSCs) of the SVZ generate not only neurons, but also
36 oligodendrocytes, the myelin-forming cells of the central nervous system.
37 Transcriptomic studies have provided detailed knowledge of the molecular events
38 that regulate neurogenesis, but little is understood about adult oligodendrogenesis
39 from SVZ-NSCs. To address this, we performed in-depth single-cell transcriptomic
40 analyses to resolve the major differences in neuronal and oligodendroglial lineages
41 derived from the adult SVZ. A hallmark of adult oligodendrogenesis was the stage-
42 specific expression of transcriptional modulators that regulate developmental
43 oligodendrogenesis. Notably, divergence of the oligodendroglial lineage was
44 distinguished by Wnt-Notch and angiogenesis-related signaling, whereas G-protein-
45 coupled receptor signaling pathways were the major signature observed in the
46 neurogenic lineage. Moreover, in-depth gene regulatory network analysis identified
47 key stage-specific master regulators of the oligodendrocyte lineage and revealed

48 new mechanisms by which signaling pathways interact with transcriptional networks
49 to control lineage progression. Our work provides an integrated view of the multi-step
50 differentiation process leading from NSCs to mature oligodendrocytes, by linking
51 environmental signals to known and novel transcriptional mechanisms orchestrating
52 oligodendrogenesis.

53 **Word count: 186**

54

55 **Keywords:** Oligodendrogenesis; Gene Regulatory Networks; Transcription Factors;
56 Signaling Pathways; Neural Stem Cell; Single Cell Sequencing.

57

58 **Main points:**

59 • Distinct adult NSC populations giving rise to either oligodendrocytes or neurons
60 can be identified by the expression of transcription factors.
61 • Gene regulatory control of oligodendrogenesis is a major fate-determinant for their
62 generation.

63

64 **INTRODUCTION**

65 Oligodendrocytes are the myelin-forming cells of the central nervous system (CNS),
66 and provide insulation for rapid axonal conduction and support to axons. In the
67 forebrain, most oligodendrocytes are generated shortly after birth from neural stem
68 cells (NSCs) of the subventricular zone (SVZ) (Azim, Berninger, & Raineteau, 2016;
69 Kessaris et al., 2006), which are also responsible for neurogenesis (Figueres-Onate,
70 Sanchez-Villalon, Sanchez-Gonzalez, & Lopez-Mascaraque, 2019), and this activity
71 is retained well into late adulthood (Fuentealba et al., 2015). The sequence of
72 oligodendroglial differentiation is relatively similar in postnatal and adult SVZ (Azim
73 et al., 2016; El Waly, Macchi, Cayre, & Durbec, 2014), whereby NSCs first generate
74 transiently amplifying progenitors (TAPs), characterized by elevated expression of
75 the transcription factor *Ascl1* (Nakatani et al., 2013), followed by progressive
76 differentiation into oligodendrocyte precursor cells (OPCs) and maturation into
77 myelinating oligodendrocytes (Azim et al., 2016; El Waly et al., 2014). In rodents,
78 approximately 5% of all cells derived from the adult SVZ are oligodendrocyte lineage
79 cells (Capilla-Gonzalez, Cebrian-Silla, Guerrero-Cazares, Garcia-Verdugo, &
80 Quinones-Hinojosa, 2013; El Waly et al., 2014; Menn et al., 2006).

81

82 Fate-mapping studies using Cre drivers under the control of regulatory regions from
83 pallial and subpallial transcription factors demonstrated that molecularly distinct SVZ
84 microdomains derive from their embryonic counterparts (reviewed in (Azim et al.,
85 2016)). The embryonic septum, the lateral ganglionic eminences, and cortex contain
86 NSCs that populate the medial (i.e. septal), ventral (i.e. striatal; also called lateral)
87 and dorsal (i.e. cortical) aspects of the adult SVZ, respectively (Azim et al., 2016;
88 Fiorelli, Azim, Fischer, & Raineteau, 2015). Localized labeling of NSCs showed that

89 regionally segregated NSCs are robustly committed to generating distinct cell
90 subtypes (Menn et al., 2006; Merkle et al., 2014; Merkle, Mirzadeh, & Alvarez-Buylla,
91 2007), and that environmental signals impinge on intrinsic fate control mechanisms
92 to modulate specific aspects of NSC and progeny behavior.

93

94 The OPC and oligodendrocyte transcriptional programs in both adult and postnatal
95 contexts have been comprehensively dissected using single cell sequencing
96 technologies (Marques et al., 2018; Marques et al., 2016; Zeisel et al., 2015). A
97 recent study revealed regional differences in lineage output from the SVZ with its
98 ventral microdomain exhibiting predominantly pro-neuronal-, and the medial wall
99 exhibiting pro-oligodendroglial hallmarks (Mizrak et al., 2019), in line with previous
100 observations using fate-mapping and transcriptomic profiling methods demonstrating
101 that ventral SVZ-NSCs during postnatal development (Azim, Fischer, et al., 2014;
102 Azim et al., 2015; Zweifel et al., 2018) and in the adult (Azim, Raineteau, & Butt,
103 2012; Dulken, Leeman, Boutet, Hebestreit, & Brunet, 2017; Llorens-Bobadilla et al.,
104 2015; Felipe Ortega et al., 2013) are biased towards olfactory bulb neurogenesis.
105 The generation of oligodendrocytes from the SVZ dorsal wall during early postnatal
106 development is, however, considered as the default source for oligodendrocyte
107 generation (Azim et al., 2017; Azim, Fischer, et al., 2014; Azim, Rivera, Raineteau, &
108 Butt, 2014; Kessaris et al., 2006). Likewise, the adult dorsal SVZ serves as an
109 additional microdomain for their generation (Azim et al., 2017; Azim et al., 2012;
110 Crawford, Tripathi, Richardson, & Franklin, 2016; Felipe Ortega et al., 2013). In
111 contrast to the number of high throughput sequencing studies defining the molecular
112 events underlying neuronal generation from adult NSC subpopulations (Marcy &
113 Raineteau, 2019), far less is known about the regulatory context of adult SVZ-

114 dependent oligodendrogenesis. This is partly due to technical limitations in isolating
115 relevant microdomains, e.g. typical SVZ whole-mount preparations are devoid of
116 dorsal SVZ tissue (Mirzadeh, Doetsch, Sawamoto, Wichterle, & Alvarez-Buylla,
117 2010). To overcome such restrictions, a cruder approach was used by capturing both
118 dorsal and lateral walls (Basak et al., 2018), which enabled us to sequence sufficient
119 numbers of single cells and to examine lineage-specific cells in the adult SVZ. Here,
120 we describe the molecular events that regulate oligodendrogenesis from the adult
121 SVZ and unravel mechanisms by which transcription factor networks and signaling
122 pathways interact to drive specification in the early oligodendrocyte lineage.

123 **Word count: 880**

124

125 **MATERIALS AND METHODS**

126 **Determining the lineage memberships of SVZ-derived single NSCs and TAPs**

127 The procedures for transgenic and FACS strategies used for capturing single cells,
128 mapping, pre-processing and RACEID are applied as described previously (Basak et
129 al., 2018). The following reporter mice were used: quiescent(q)NSCs, few active(a)
130 and primed(p)NSCs were taken from Troy:::GFP mice; TAPs and neuroblasts were
131 harvested from Ki67:::RFP mice, and qNSCs (including a few pNSCs and aNSCs)
132 were extracted from Ki67:::creRT2:::Tom2 mice. FACS analysis (Figure S1a) allowed
133 identification/isolation of GLAST+/EGF- qNSCs, GLAST+/EGF+ aNSCs, GLAST-
134 /EGF+ TAPs and O4+ oligodendrocytes. Parameters for cell clusters identification
135 were adapted as done previously (Basak et al., 2018) to obtain SVZ-lineage specific
136 clusters.

137

138 We predicted that the transcriptional hallmarks of oligodendrogenesis and
139 neurogenesis from the postnatal SVZ microdomains are retained to a certain extent
140 into adulthood. Bulk datasets of our previous study (Azim et al., 2015) were used for
141 identifying transcriptional signatures of the entire oligodendrocyte lineage by
142 comparing dorsal NSCs, dorsal TAPs and oligodendrocytes and for ventral SVZ-
143 derived neurogenesis. Transcription factors used as markers for lineage
144 identification in adult single cell were (i) highly expressed during early postnatal
145 development and (ii) uniquely expressed in either oligodendrocyte or neuronal
146 lineages. These included among other genes *Notch2*, *Epas1*, *Foxo1*, and *Esrrg2*. A
147 first characterization was performed with RACEID to identify rarer cell populations in
148 single cell sequencing (Grun et al., 2015), then PartekFlow®
149 (<http://www.partek.com/partek-flow/>) was used to assign single cells to defined SVZ
150 lineages, including the rarer ones from RACEID. Visual inspection of t-Distributed
151 Stochastic Neighbor Embedding (tSNE) plots displaying transcript levels for selected
152 lineage-specific markers was used to sub-cluster cells found in close proximity in the
153 plots. Figure S1b contains examples of some of the markers used in this
154 oligodendrocyte lineage detection step.

155
156 Transcription factor markers obtained from bulk datasets were used to identify single
157 cells of the oligodendroglial lineage (Azim et al., 2015), aside from OPCs and mature
158 oligodendrocytes within subpopulations of NSCs/TAPs (Figure S1b). The soundness
159 of our lineage membership assessment was further evaluated by comparing the
160 gene expression profile of the remaining cells, expected to belong to the larger
161 neurogenic population, with bulk datasets of adult qNSC/aNSC/TAP/NB populations.
162 Adult TAPs and neuroblasts we described in a recent study (Azim et al., 2018).

163 PartekFlow was used to generate heat PCA plots describing pallial and subpallial
164 marker expression by cells in the early stages of the oligodendrocyte lineage
165 (qNSCI, qNSCII and pNSC). Gene Specific Analysis algorithm from PartekFlow was
166 used with default parameters for acquiring gene lists defining the distinct cell
167 lineages. Lineage-specificities were considered statistically relevant if the
168 corresponding *p*-values were below 0.05. An additional analysis for determining the
169 expression signatures of common genes (shared between oligodendroglial and
170 neuronal lineages) was performed by identifying cluster-enriched genes for the first 5
171 stages of differentiation (qNSCI-to-TAP) without separation of lineage-specific
172 clones. The above steps allowed the definition of a total of 13 clusters: qNSCI,
173 qNSCII, pNSC, aNSC, TAP, neuroblasts for the neuronal lineage and OLqNSCI,
174 OLqNSCII, OLpNSC, OLaNSC, OLTAP, OPC and mature oligodendrocytes for
175 oligodendroglial lineage.

176
177 Differential expression analysis was performed using datasets mentioned above by
178 applying methods as described in (Azim et al., 2018) in addition to the cluster
179 enriched transcripts using the Seurat V3 package as described in the next
180 paragraph. Genes were filtered to select for transcription factors or transcriptional
181 cues identified with PartekFlow. Macro-groups accounting for distinct differentiation
182 stages were characterized as follows: (i) early oligodendrocyte group and the
183 neurogenic group were defined by their expression of transcription factors expressed
184 in single cells of (OL)qNSCI, (OL)qNSCII and (OL)pNSC; (ii) mid group for either
185 lineage included transcription factors expressed in aNSCs and TAPs. The same
186 datasets were used to identify enriched transcription factors when specific
187 differentiation stages were compared. Precisely, the following stages were examined

188 as follows: (1) dorsal NSCs vs dorsal TAPs, OPCs, immature oligodendrocytes and
189 mature oligodendrocytes; (2) dorsal TAPs vs dorsal NSCs, OPCs, immature
190 oligodendrocytes and mature oligodendrocytes; (3) vNSCs vs vTAPs, TAPs and
191 neuroblasts; (4) vTAPs vs vNSCs, TAPs and neuroblasts; (5) qNSCs vs aNSCs,
192 TAPs and neuroblasts; (6) aNSCs vs qNSCs, TAPs and neuroblasts. Statistical
193 analysis was performed using ANOVA for determining the differentially expressed
194 (DE) transcription factors. Comparison of adult transcription factor expression in
195 postnatal NSCs was summarized by assigning each transcription factor to a
196 category: “1” indicates upregulated and highly expressed transcription factor, “-1”
197 downregulated transcription factors, while “0” represents the remaining ones.

198

199 **Clustering and visualization of single cell data using the Seurat R package**

200 The R package Seurat V3 was used to process single cell transcriptomic data and
201 elucidate their heterogeneity (<https://satijalab.org/seurat/vignettes.html> (Butler,
202 Hoffman, Smibert, Papalexi, & Satija, 2018)). Single cells were assigned a unique
203 identifier, then the default pipeline for analysis was performed: data were log-
204 normalized and cells containing mitochondrial genes with a *p*-value greater than 0.05
205 were filtered out. The obtained matrix was scaled so that JackStraw function could
206 be applied for comparing the *p*-values distribution for all principal components. Using
207 the genes displaying higher variation among the 13 clusters identified with
208 PartekFlow, the Seurat function FindVariableFeatures determined 7 oligodendroglial
209 and 6 neuronal clusters that were employed for the downstream pseudotime
210 analysis. Graphical representations were created using Seurat package. Differential
211 gene expression analysis was performed with FindAllMarkers function applying
212 Wilcoxon rank sum test to find transcriptional markers of the 13 clusters. Of note,

213 several statistical tests were implemented to ensure the reliability of the set of most
214 relevant genes. Aside from DESeq2, differentially expressed genes across these
215 methods were comparably similar (further detailed in
216 https://satijalab.org/seurat/v3.0/de_vignette.html).

217

218 **FateID cellular trajectory construction**

219 The genes specific for the 13 clusters were processed for assessing lineage biases
220 by using FateID package for R environment. The goal is to resolve early lineage
221 priming via iterative random forest classification (Herman, Sagar, & Grun, 2018). The
222 default settings of the package were applied. In order to determine the relationship
223 between terminal differentiation states and naïve stem/progenitor states, mature
224 oligodendrocytes were equated as the heterotypic outlier of the neurogenic lineage.
225 The variable genes in the neurogenic clusters and mature oligodendrocytes were
226 used as a subset expression data frame. The top 10 genes belonging to each cluster
227 as determined by the above Seurat analysis were used as learning set for the
228 classification method hence defining the v matrix, while neuroblast and mature
229 oligodendrocyte clusters were indicated as target set. Using fateBias function, a few
230 iterations were operated by comparing consecutive stages of differentiation by
231 setting the training set as the previous stage and the test set as the following one.
232 For example, the defined NSC/TAP pool of the oligodendroglial lineage (including
233 neuroblasts) was used as training set and mature oligodendrocytes, OPCs and
234 neuroblasts were classified as the test set. Differentiation trajectories were computed
235 using the principal curve function “prc”. The dimensionality reduction coordinates of
236 the analyses of the cells and differentiation trajectories (data contained in the “dr”

237 and “pr” lists) were exported and plotted using the ggplot2 R package for improved
238 graphical representation.

239

240 **Cell cycle regression**

241 NSCs/TAPs/neuroblasts, quiescent or activated, were further investigated to
242 determine their position within the cell cycle, using CellCycleScoring function of
243 Seurat package. Full details are available at
244 https://satijalab.org/seurat/v3.0/cell_cycle_vignette.html (Butler et al., 2018). Seurat
245 estimates the mean expression of the marker genes from 43 S-phase and 54 G2/M-
246 phase thus generating a uniform rank for S- and G2/M-phase for each cell, which
247 results in the assignment of each single cell to a particular phase. The score was
248 gauged by deducting the mean expression of the 10 nearest neighbor-cells in
249 dimensionality reduction space computed by Seurat. Cell cycle scorings of cell
250 populations were plotted according to their pseudotime trajectory coordinates as
251 previously calculated. The data are visualized as cell cycle marker signal distribution
252 in ridge plots (Figure 3). The aNSCs and TAPs of both lineages were further
253 classified according to the different phases of the cell cycle, therefore leading to the
254 identification of 15 distinct clusters (while the initial aNSC and TAP clusters were
255 replaced). Seurat was run generating cluster-enriched expression profiles and those
256 of the mid stages were used for further GO analysis as described below.

257

258 **Gene ontology and pathway annotation of cell clusters**

259 Gene lists for the original 13 clusters and the additional 4 ones (Figure 3e) were
260 used for overrepresentation analysis using Protein ANalysis THrough Evolutionary
261 Relationships (PANTHER) analysis tools (<http://www.pantherdb.org>) (Mi, Poudel,

262 Muruganujan, Casagrande, & Thomas, 2016)). Comparing the overrepresented
263 pathways of the oligodendroglial and neuronal clusters, PANTHER pathways
264 function was used for pointing out the mechanisms that differ or are shared between
265 stages within a lineage or between the same stage in oligodendroglial and neuronal
266 lineages. In this analysis, a minimum of 4 pathways for each cluster was retained if
267 the corresponding *p*-value was below 0.05. TAP clusters or the later stage
268 OPCs/mature oligodendrocytes contained a greater number of highly expressed
269 genes, and so the top 10 most significantly expressed genes found with Seurat were
270 used. Identification of genes that are unique to the oligodendrocyte lineage, the
271 neuronal lineage and the shared ones was performed using the R Package Venn
272 Diagram and the online tool <http://www.biovenn.nl/index.php>. Pathway and Protein
273 Class lists obtained from PANTHER were downloaded for the analyses described
274 above and presented as dot plots using the ggplot2 R package. Similarly, the time
275 courses for GO SLIM Biological Processes were constructed for the oligodendrocyte
276 lineage using the 5 most significant terms. Pathway time course was represented
277 applying the same method and using selected key pathways from the prior analysis.

278
279 Due to the potential reversibility of early (i.e. NSC) cell state transitions (Basak et al.,
280 2018; Calzolari et al., 2015; Obernier et al., 2018), a considerable overlap among
281 cell clusters in terms of expression profiles, Reactome and PANTHER Pathways,
282 and Protein Class led to the definition of 3 broader groups. For this, the earlier
283 stages constituting OLqNSCI, OLqNSCII and OLpNSC, the mid stages represented
284 by OLaNSC and OLTAP, and the remaining OPCs and mature oligodendrocytes as
285 the later stages were assembled. Results for signaling Pathways, Reactome and
286 Protein Classes enrichment corresponding to the 3 groups were merged and the top

287 third most significant terms for each of the 3 groups were charted as dot plots and
288 ranked in descending order based on their enrichment. Results for transcription
289 factor Protein Class for the 7 oligodendrocyte lineage clusters were visualized with a
290 heatmap representing the top 3 most enriched PANTHER Pathways related to
291 “transcription factor function” across the 7 clusters. The heatmap was obtained with
292 the pheatmap package in R.

293

294 **Characterizing transcription factors for gene regulatory network (GRN)
295 reconstruction**

296 Once the most significant set of genes is determined, it is of importance to
297 investigate if and how the genes are interacting at the molecular level. In addition to
298 the genes previously identified as transcription factors, additional transcription
299 factors known to play a central role in NSC differentiation were selected and their
300 putative targets taken from http://genome.gsc.riken.jp/TFdb/tf_list.html,
301 <http://www.tfcheckpoint.org/index.php/browse>, and PANTHER. Given the large
302 numbers of transcription factors identified, a prioritization procedure was developed,
303 relying on functional and transcription factor-transcription factor interaction data.
304 Initially, the Cytoscape app GeneMANIA was used to identify functional interactions
305 among the input genes (Franz et al., 2018). The data available for GeneMANIA for
306 human gene orthologs are significantly more numerous and better characterized,
307 therefore, mouse gene symbols were converted to human gene symbols. The genes
308 used as input for GeneMANIA were limited to transcription factors and the queries
309 were performed using the default parameter besides the type of interactions. In fact,
310 the selected databases were “genetic” for downstream gene regulation and
311 “physical” for protein-protein interactions. A first network (precursor to the one

312 depicted in Figure S7) was thus obtained, on which additional analyses were
313 performed for prioritizing the large numbers of transcription factors included. For this,
314 the heat diffusion algorithm was applied (Carlin, Demchak, Pratt, Sage, & Ideker,
315 2017) to facilitate identification of central transcription factors according to their level
316 of interactions: the higher the number of interactions, the higher the calculated heat
317 diffusion rank. The heat diffusion algorithm was applied 3 times separately, once
318 focusing on genetic interactions, (Figure S7b), once on physical interactions (Figure
319 S7c), and finally combining the newly obtained heat diffusion ranks (Figure S7a).
320 The diffusion ranking values so obtained were plotted against the number of
321 interactions of each transcription factor. As additional information, the nodes size of
322 the included transcription factors was adjusted to their combined physical and
323 genetic interaction ranks in Figure S7d.

324

325 Aiming to group the transcription factors to organize the network similarly to the
326 clustering of FateID, the precursor network was organized to depict transcription
327 factor expression according to their stage of expression. The primary goal is focusing
328 on oligodendrogenesis, hence transcription factors whose annotation showed an
329 enrichment towards neuronal lineage only were discarded. Genes common to both
330 lineages at different stages were processed in order to define transcription factors
331 that show specificity to either lineage. The specificity threshold was defined at linear
332 2-fold. This selection enabled emphasizing genes/transcription factors that are
333 expressed in the oligodendrocyte lineage still including those ones sharing neuronal
334 signatures. To assign transcription factors to the appropriate oligodendrocyte or
335 neuronal clusters, the principle of higher expression was adapted. Nodes and labels
336 sizes were organized based on the FDR values. A separate grouping of transcription

337 factors was made by selecting the transcription factors overlapping between aNSCs
338 and TAPs. Transcription factors that were significantly expressed in at least 2
339 different stages of the oligodendrocyte lineage were classified as "Pan transcription
340 factors". GeneMania networks presented in Figure S7a were used as visual aids for
341 facilitating the positioning of transcription factors according to the stages in
342 differentiation they are expressed in.

343

344 **TETRAMER reconstruction of GRNs of SVZ lineages**

345 The above step focuses on transcription factor functions in terms of their genetic
346 transcription factor-transcription factor interactions. This information was used as the
347 framework for a comprehensive inspection of transcription factor-target gene
348 interactions. For unravelling GRNs, TETRAMER (TEmporal TRAnscription regulation
349 Modeller) reconstructs fate transition-specific GRNs by integrating transcriptome
350 data (user provided) with inbuilt information (Cholley et al., 2018) (available gene
351 expression profiles, human genome-wide promoters and enhancers maps, and
352 ChIP-Seq available datasets) (see also <http://ngs-qc.org/tetramer/>). The input data for
353 TETRAMER was constituted of a matrix containing 1467 genes – including
354 transcription factors – irregularly expressed in the oligodendrocyte lineage during
355 differentiation and, at the same time, expressed more in the neuronal lineage. Part of
356 the genes were included in the input matrix due to their association with GO
357 Biological Processes identified as major hallmarks of later stages of oligodendroglial
358 maturation. These hallmark GO Biological processes were: (i) Signal Transduction,
359 (ii) Ca Ion Transport, (iii) Synaptic Organization, (iv) CNS Development, and (v)
360 Multicellular Organismal Development. All of them presented a *p*-value < 0.0002 (as
361 estimated with Hypergeometric test). Specific hallmarks for mature oligodendrocytes

362 in the considered GO Biological Process were: (i) Cytoskeleton Organization, (ii)
363 Myelination, (iii) Myelin Maintenance, (iv) Cell Adhesion, and (v) Transport. All of
364 them presented a *p*-value < 0.007 (as estimated with Hypergeometric test). Genes
365 consistently enriched more than 2.5 folds (aside from transcription factors) in OPCs
366 and mature oligodendrocytes in the lists above and among DEGs found with
367 Seurat were considered for a further functional enrichment analysis using the freely
368 available Functional Enrichment analysis tool (FunRich) <http://funrich.org/index.html>.
369 GO Biological terms were reduced to fit, and a complete list has otherwise been
370 made publicly available (see below).

371

372 The following settings were necessary prior to assessing the transcriptional signaling
373 propagation in the GRNs with TETRAMER. The matrix consisting of 1467 genes,
374 among which are transcription factors expressed in both lineages (common
375 transcription factors) or exclusively in either lineage, was used to construct 3
376 separate subnetworks (presented in Figure 4b-d). These networks were filtered
377 accordingly to highlight transcription factors expressed in the neuronal lineage and
378 excluding genes expressed in OPCs and mature oligodendrocytes. The nodes
379 expressed in the qNSCI stages were named “start node” as they represent the initial
380 time point of differentiation, and transcription factors expressed in more than 2
381 stages were termed “pan transcription factors”. The nodes expressed in final stages
382 of differentiation, i.e. OPCs and mature oligodendrocytes for the oligodendrocyte
383 lineage, were named “end node”. The time course for differentiation was arranged in
384 order from qNSCI to mature oligodendrocytes, and all intermediate differentiation
385 stages were selected for network propagation. In the TETRAMER results section, all
386 transcription factors containing a yield were considered to be part of the main

387 signaling network. When the signal propagation network viewing was initiated, nodes
388 in the network were colored from white/light red for the qNSCI nodes to darker red
389 for mature oligodendrocytes, white to dark grey for transcription factors expressed in
390 both lineage as "common transcription factors", and white to dark blue for
391 transcription factors expressed in the neuronal lineage. Node sizes in these networks
392 and subsequent analysis were graded based on the heat diffusion rank combined
393 with additional parameters: node stress (calculated as the number of shortest paths
394 passing through the considered node) indicating the extent of node activity,
395 neighborhood connectivity, and the numbers of transcription factor-target gene
396 interactions (edges). The values for each of these criteria were normalized in the
397 range (0, 10) (low to high attribute values) and an average of all parameters was
398 computed generating a final score termed as the connectivity index.

399

400 **Reconstruction of the AdultOLgenesis GRN**

401 The GRNs representing transcription factors expressed in the oligodendrocyte
402 lineage and the ones common to both SVZ lineages were examined further by
403 combining data of these two networks. The input matrix used for TETRAMER was
404 expanded with genes that account for the GO Biological Processes for later stages
405 of oligodendrogenesis. The TETRAMER analysis was performed as described
406 above. The newly obtained larger network was expanded further to include the
407 interactions with transcription factors known to play a central role in NSC
408 differentiation. Additional ChIP-seq data for *Ascl1*, *Cebpa*, *Hdac2*, *Jun*, *Sox4*, *Sox9*,
409 *Tgif2*, and *Tpr53* were obtained from the Chip Atlas database (Oki et al., 2018), while
410 *Hopx* (He et al., 2016; Jain et al., 2015), *Zeb1* (Rosmaninho et al., 2018) were taken
411 from individual studies. For *Trp53* and *Zeb1* original data, the potential targets were

412 annotated using human species gene names, hence to merge the results of the
413 different datasets coherently, an R script was compiled for converting human-
414 annotated to mouse-annotated genes (biomaRt package) (Durinck, Spellman,
415 Birney, & Huber, 2009). For the potential gene targets extracted from the Chip Atlas
416 database, a threshold on the score returned by the database was defined to select
417 the targets with highest level of confidence (threshold values: 250). For *Hopx*, a
418 different thresholding approach was applied, for the available data were processed
419 differently: ChIP-seq data were processed with the Homer suit of tools, and therefore
420 a different score was assigned to each identified peak. To discriminate between the
421 relatively reliable targets, the average score was calculated and set as the
422 discriminant threshold. For all the added transcription factors, a node was added to
423 the precursor GRN representing the transcription factor itself. Interactions
424 representing the ChIP-Seq data were created between the transcription factor and
425 the targets already included in the precursor GRN. In order to select the target genes
426 and generate this representation, a Python script was compiled. The code generated
427 a text file associating to each transcription factor-target pair the source of the datum,
428 the type of the interaction, and the type of the source data. To extend the number of
429 interactions of the GRN specifically or oligodendrogenesis, the transcription factor-
430 target gene networks were imported independently in Cytoscape and union-merged
431 with the Exploration network recently published by Cantone and colleagues
432 (Cantone et al., 2019). The union merge was repeated between the latest union
433 merge and the AdultOLgenesis Network generated by TETRAMER, thus
434 incorporating additional information. For the 11 selected transcription factors, targets
435 were selected based on (i) a score describing the confidence of the actual formation
436 of the transcription factor-target gene binding, thus increasing the reliability of the

437 interaction, and (ii) the biological context of the transcription factor-target gene
438 binding by limiting the set of genes to the ones previously identified in the Core GRN.
439 The confidence in the identification of the same transcription factor-target gene
440 binding in human and mouse species is ensured by a high level of genomic
441 similarity.

442
443 The obtained network was remodeled for positioning the nodes according to their
444 pseudotime trajectory coordinates, thus providing an improved overview for
445 transcriptional processes. The GeneMania network presented in Figure S7a was
446 used as reference to guide the correct placement of genes in individual stages of
447 differentiation. The Cytoscape plugin CoordinatesLayout version 3.0 and
448 copycatLayout version 0.0.9 were used. The average coordinates for defined cells at
449 each stage of differentiation was calculated along its x-y axis, and at each of the
450 estimated positions, a node was added to represent the corresponding differentiation
451 stage. The size of the node was scaled to reflect the relative abundance of
452 transcription factors associated to the differentiation stage. The “mock” nodes
453 representing oligodendrocyte cell clusters were organized according to their FateID
454 trajectories. Nodes representing transcription factors/genes associated with each of
455 the different stages of the oligodendrocyte lineage were grouped together and force
456 directed using Compound Spring Embedder (CoSE), and overlaid with the mock
457 nodes. Settings for CoSE were adjusted systematically for all oligodendrocyte stages
458 with edge lengths kept constant and spring strength/repulsion adjusted equally.
459 Nodes with higher heat diffusion ranks were permitted to overlay those genes with
460 lower heat diffusion ranks to highlight transcription factors with greater functional
461 relevance. Interactions were bundled using handles with the following parameters:

462 0.003 spring constant, compatibility threshold of 0.3 and 500 maximum iterations.
463 Nodes without interactions (that is, without edges) were excluded and hidden in the
464 background. Summaries highlighting downstream transcriptional regulation
465 (outwards transcriptional propagation) were constructed by adjusting node and edge
466 sizes reflecting the relative numbers of transcription factors/genes in the different
467 stages of differentiation and the downstream activation or repressive transcriptional
468 control, respectively. Five additional GO Biological Processes were manually
469 included close to later-stage oligodendrocytes. The entire reconstructed network was
470 termed “AdultOLgenesis GRN” and was thus an expansion of a recent study
471 describing GRNs during OPC-to-mature oligodendrocyte differentiation (Cantone et
472 al., 2019) by inclusion of additional regulatory features.

473

474 **Assessing transcriptional propagation by selected transcription factors and**
475 **Signaling Pathways**

476 Transcription factors expressed in defined stages of oligodendrogenesis (see also
477 Figure S7) or associated in PANTHER pathways were tested for transcriptional
478 propagation across the Core GRN (see also Section 7 of the online repository:
479 <https://github.com/kasumaz/AdultOLgenesis>). The transcription factors were selected
480 with their direct target genes and subsequent secondary and tertiary target genes.
481 All primary target genes were retained, whereas secondary and tertiary target genes,
482 if they were transcription factors, were filtered according to their protein-protein
483 interaction and connectivity index of >7.5 and >7, respectively. Biological Process
484 GO terms were preserved throughout. Interactions of transcription factors associated
485 with PANTHER pathways, secondary and tertiary target genes were sized in order of
486 line thickness in this order. Manual curation was operated for correcting the edges

487 between GO Biological Processes and PANTHER pathways. Transcription factors in
488 each network were ranked in heatmaps for each pathway, according to the number
489 of target gene interactions (activation/inhibition) across the different pathways
490 selected for analysis. Gene regulatory data for the quantification of activation,
491 inhibition and unspecified interaction were obtained from the edge section of the
492 AdultOLgenesis GRN in Cytoscape.

493 **Word count: 3860**

494

495 **RESULTS**

496 **Identification of the earliest stages of the SVZ-derived oligodendrocyte lineage**

497 Transcriptional networks controlling oligodendrogenesis from adult SVZ-NSCs are
498 currently unsolved. Here, NSCs/progenitors and subtypes of neural cells found within
499 the young adult SVZ were isolated and FACS-enriched using genetic reporters and
500 immunochemical markers, as described in a previous report on adult neurogenesis
501 (Basak et al., 2018) (Figure S1a). Relying on well-established markers for the earlier
502 stages in oligodendrogenesis as a guide, we identified putative lineage-specific
503 subpopulations of NSCs (Figure S1b). Approximately 1200 single cells were
504 visualized using tSNE plots and used for categorizing previously defined clusters and
505 subclusters (Basak et al., 2018). We hypothesized that, as in the early postnatal
506 SVZ, adult lineage-specific NSCs could be identified by their expression of
507 oligodendroglial and neuronal hallmark genes. To this end, previously generated lists
508 of genes associated with SVZ-oligodendrogenesis from bulk datasets were
509 assembled and searched for oligodendrocyte lineage-enriched genes when
510 compared to neurogenic populations (Azim et al., 2017). In this initial step,
511 PartekFlow was used to input a number of landmark genes that define the earlier
512 stages of the oligodendrocyte lineage. These include the essential transcription
513 factors *Olig2*, *Olig1* and *Sox10*, and a cohort of other transcription factors as
514 described in Materials and methods (Figure S1b). As an advantage, PartekFlow
515 highlights cells based on input gene marker profiles, allowing the identification of
516 neighboring cells that are transcriptionally similar. Following classification of putative
517 oligodendrocyte lineage cells descending from NSCs/TAPs, gene lists derived from
518 PartekFlow had initially revealed that the major differences in the 2 SVZ lineages are
519 attributed to the expression of transcription factors (see below), in agreement with

520 the observed pre-eminence of transcription factors as lineage-specific markers within
521 postnatal gliogenic lineages (Azim et al., 2015). Thus, expression levels of
522 transcription factors were explored. In particular, single NSCs/TAPs expressing the
523 above 3 essential transcription factors, as well as a cohort of others (Figure S1b)
524 expressed in postnatal gliogenic NSCs were identified as likely to contribute to the
525 oligodendrocyte lineage (Figure 1a) and amounted to approximately 7.2% of all
526 NSC/TAPs across the 5 NSC and TAP stages of differentiation, which is in line with
527 previous reports describing the relative scale of SVZ-oligodendrogenesis when
528 compared to the generation of neurons (Menn et al., 2006). This particular
529 subpopulation is identified by the co-expression of the known pan-NSC marker *Hes5*
530 in qNSCs I/II expressing *Olig2* (Figure 1b). The first 3 stages of identified OLNSCs
531 also expressed the pallial marker *Pax6* whereas they did not express the ventral
532 SVZ markers *Gsx2* and *Nkx2-1* (Figure 1b). Most notably, an initial analysis of
533 differentially expressed genes (DEGs) revealed patterns that are reminiscent of
534 transcriptional programs found during postnatal oligodendrogenesis (Figure S1b).
535 Identified cells of the oligodendrocyte lineage in the adult cluster closely with
536 corresponding pooled populations (qNSCI-pNSC) in transcription factor expression,
537 including postnatal gliogenic NSCs/TAPs (Figure S1c), reinforcing the view that
538 subsets of adult NSCs are committed to an oligodendrogenic fate.

539
540 Next, FateID pseudotime analysis was performed to assess whether identified
541 putative oligodendrogenic and neurogenic NSCs define distinct cell state trajectories
542 (Herman et al., 2018). The genes that are significantly varying as determined by the
543 Seurat analysis (see Materials and methods) in oligodendrogenic and neurogenic
544 lineages, and the genes enriched in mature oligodendrocytes, were used for testing

545 the hypothesis that the selected oligodendrocyte lineage cells engage in a trajectory
546 from earlier subpopulations of NSCs/TAPs. Oligodendrocytes and neuroblasts were
547 used as the final lineage endpoints. Neuroblasts followed a continuous trajectory
548 from qNSCI and many neurogenic TAPs resembled neuroblasts in pseudotime
549 (Figure 1c). Addition of mature oligodendrocytes to this mostly neurogenic trajectory
550 forces an early branching for the oligodendrocyte lineage, at qNSCI/II stages.
551 However, when considering mature oligodendrocytes alongside putatively
552 oligodendrogenic NSCs/TAPs and OPCs, mature oligodendrocytes branched off the
553 main trajectory closer to OLaNSCs, TAPs and OPCs. Interestingly, addition of
554 neuroblasts to the oligodendroglial trajectory resulted in a transcriptional path that
555 overlapped partly with fewer OLTAPs compared to the neurogenic TAPs, highlighting
556 the distinction between the two lineages. Genes detected in early- to mid-stage
557 oligodendrocyte lineage cells (qNSCI to TAPs; Figure 1d-f) regulate signaling-to-
558 transcriptional control of the oligodendrocyte lineage. Cluster-enriched markers
559 (Figure 1f) include genes coding for the G-protein-coupled receptor genes *Lrig1* and
560 *Adora2b* for OLqNSCI (Poth, Brodsky, Ehrentraut, Grenz, & Eltzschig, 2013; Simion,
561 Cedano-Prieto, & Sweeney, 2014); the Bmp4-responsive gene *Htra1* serine protease
562 (Chen et al., 2018), and the gliogenic transcriptional adaptor *Hopx* for OLqNSCII
563 (Zweifel et al., 2018); the transcriptional regulator *Foxo1* (Kim, Hwang, Muller, &
564 Paik, 2015), or the mitochondrial ketogenic enzyme *Hmgcs2* in OLpNSCs (Jebb &
565 Hiller, 2018). OLaNSC and OLTAP markers include genes encoding for *Hspa1a* and
566 *Hspa1b*, and *Cdk4* and *Hes6*, respectively (Arion, Unger, Lewis, Levitt, & Mirmics,
567 2007; Kim et al., 2015; Lukaszewicz & Anderson, 2011). This analysis revealed that
568 many of the cluster-specific genes belong to families involved in signaling and
569 transcriptional control, and demonstrated that cells representing the earliest stages

570 of the oligodendrocyte lineage are identifiable among NSCs, allowing the analysis of
571 lineage-specific signatures. Further examples of pan lineage markers are given in
572 Figure S2.

573

574 **Stage-specific processes**

575 Following determination of stage-/cluster-specific signatures, we focused on
576 individual lineages (oligodendrocyte and neuronal, separately) and analyzed the cell
577 clusters in each (7 oligodendroglial clusters, 6 neuronal clusters) for pathway
578 enrichment using the PANTHER database. The most significant pathways for each
579 stage of the 2 lineages are illustrated in dot plots showing the activity of a given
580 pathway across the different clusters (Figure 2a). In this analysis, the genes
581 exclusively belonging to 1 cluster were examined. Interestingly, the earliest stages of
582 the oligodendrocyte lineage (qNSCI-pNSC) were uniquely characterized by the
583 activity of pathways (e.g., “angiogenesis”, “cysteine biosynthesis”, “cytoskeletal
584 regulation by RhoGTPases” and “pyruvate metabolism”), which also distinguished
585 them from early NSC stages of the neuronal lineage. Contrastingly, a considerable
586 overlap in pathways in the mid-stages (aNSC and TAPs) between the 2 lineages
587 was evident, with few exceptions such as “Notch signaling” that was prominently
588 enriched in OLaNSCs, and “p53 and cell cycle pathways” enriched in the same
589 stages of the neuronal lineage.

590

591 All genes enriched in the oligodendrocyte lineage clusters (including those shared
592 with the neuronal lineage) were next examined for characteristic biological processes
593 (Slim Biological Processes in PANTHER) and plotted across the various stages of
594 lineage progression. Machineries related to “lipid or energy metabolism”, “response

595 to signaling" or "developmental patterning molecules" were enriched in the earlier
596 stages, whereas mechanisms such as "translation", "gene expression" and "cell
597 division" were most prominent in OLaNSCs and OLTAPs (Figure 2b), consistent with
598 previous observations (Llorens-Bobadilla et al., 2015). At a later stage of
599 differentiation, OPCs engage in processes that were also active in OLqNSCII. For
600 example, GO biological process "cell communication" is enriched in OLqNSCII, and
601 then again at the OPC stage (Figure 2b), possibly accounting for the close proximity
602 of these 2 segregated populations in both the tSNE plots and pseudotime (Figure
603 1a,c). Many of the characteristic processes detected in mature oligodendrocytes
604 increase in expression during the course of lineage progression. We expanded this
605 analysis for both protein class and signaling pathways, to include the neuronal
606 lineage (Figure S3), observing that transcription factors and nucleic acid-binding
607 proteins are highly abundant in the early and mid-stages of the oligodendrocyte
608 lineage along with major developmental pathways. A time course for the expression
609 of the most significant signaling pathways in this analysis points to key processes
610 regulating transition along the oligodendrocyte lineage (Figure S4), with increasing
611 transcriptional activity suggested by the pattern of expression of transcription factors
612 and nucleic acid-binding proteins across the different oligodendrocyte lineage stages
613 (Figure S5). Altogether, these findings outline potential mechanistic differences in the
614 control of progression within the 2 SVZ-derived lineages, with notable differences in
615 inferred signaling pathway activities and in the expression of transcriptional
616 modulators.

617

618 **Cell cycle properties of SVZ-NSCs/progenitors**

619 Given the observed differences in cell cycle, transcriptional control and nucleic acid
620 synthesis pathways in mid-stages (OLaNSC, OLTAP) of the oligodendrocyte lineage
621 we further explored stage-specificity. To this end, cell clusters were analyzed by
622 computing cell cycle phase scores based on canonical markers for the 3 main cycle
623 phases (S, G2M and G1 phase) using the Seurat V3 package. Single cells'
624 expression levels of established cell cycle markers were compared and data were
625 regressed out by modeling the relationship between expression signatures of each
626 cell with cell cycle markers. Upon identification of the predicted cell cycle state for
627 cells of all 13 clusters, those representing the oligodendrocyte lineage were plotted
628 in accordance to their pseudotemporal coordinates and summarized in bar plots for
629 both lineages (Figure 3a,b), and signal intensities as ridge plots (Figure 3c). In both
630 lineages, the early stage NSCs (qNSCI-pNSC) and OPCs were almost entirely at the
631 G1 phase with signal intensities shifted towards baseline, whereas S and G2M
632 marker signals were detected in neuroblasts (Figure 3c). More than half of the
633 aNSCs in either lineage were actively cycling and rarely at the G2M phase, whilst the
634 remaining were quiescent. Although no proneuronal TAP was found to be quiescent,
635 with just over 55% at the G2M phase and the remaining in S phase, a slightly greater
636 proportion of OLTAPs were in S phase. Signal intensities for the S and G2M markers
637 were relatively absent in the early neuronal lineage.

638

639 Following identification of the mid-stage cell cycle properties, Seurat V3 was used to
640 identify cluster-specific genes in OLaNSCs and OLTAP by subclassification
641 according to their predicted cell cycle phase. Therein, transcripts significantly
642 expressed by the 9 cell clusters (OLqNSCI, OLqNSCII, OLpNSC, OLaNSC in G1,
643 OLaNSC in S Phase, OLTAP in G2M, OLTAP in S Phase, OPC and mature

644 oligodendrocytes) were extracted and a further pathway analysis was performed on
645 the mid-stages of the oligodendroglial lineage (OLaNSC in S Phase, OLTAP in G2M
646 and OLTAP in S Phase). Pathways and Protein Class determination was performed
647 for OLaNSCs in the G1 and S phase in the intercept (genes overlapping in the 2
648 groups) in this analysis and the same for G2M and S phase for OLTAPs (Figure 3d,
649 e). Interestingly, aside from Notch and Hedgehog signaling, metabolic-like
650 mechanisms that include thiamine metabolism and threonine biosynthesis are also
651 features of quiescent OLaNSCs, whereas cycling aNSCs were characterized by
652 pathways regulating transcription, translation, and nucleic acid binding. In OLTAPs at
653 the G2M phase, EGF-, p38 MAPK-, p53 and interferon gamma-signaling were
654 significantly enriched. Furthermore, as expected, many of the pathways expressed in
655 actively cycling TAPs included regulation of mRNA, replication, and cell cycle-related
656 processes (Figure 3d). Cell cycle-related analysis of mid-stage oligodendrocytes
657 accordingly revealed that the major protein classes expressed in G2M and S phases
658 were “nucleic acid-binding” and “transcription factor”, whereas OLaNSCs in G1 were
659 characterized by extracellular matrix and vesicle-associated SNARE proteins (Figure
660 3e). Altogether, examining heterogeneity of cell cycle states in proliferative cells of
661 the oligodendroglial lineage suggests that transcriptional cues are a major driver in
662 OLqNSCII and in mid-stages of the lineage, which warrants further investigation.

663

664 **Gene regulatory networks in NSCs/TAPs driving myelination**

665 The previous analysis disclosed major classes of genes expressed in earlier
666 oligodendroglial lineage cells, notably with mid-proliferative cell stages featuring
667 abundant expression of transcriptional modulators. Therefore, the expression of
668 transcription factors (including transcriptional adapters and transcription cofactors)

669 was further explored in both the oligodendroglial and neuronal lineages.
670 Transcription factors were prioritized via a GeneMania-based genetic and physical
671 interaction analysis. This step facilitates predicting the effects of genetically
672 perturbing a given transcription factor, in terms of its impact on neighboring genes,
673 based on predicted transcription factor-to-targetgene interactions and protein-protein
674 interactions (see Materials and methods; Figure S6). To determine which
675 transcription factors are most relevant according to their genetic perturbation, genes
676 were prioritized by applying the “heat diffusion” algorithm that tests the input query
677 data and the functional interaction of each gene for propagation across the network.
678 Strongly connected nodes in the network, supporting sufficient regulatory activity
679 propagation, are uncovered and allow creation of subnetworks, enabling exclusion of
680 nodes with lower functional relevance. Prioritization steps were applied for both
681 physical (protein-protein interactions) and genetic interaction (Figure S6a and
682 expanded further in Figure S7) and identified transcription factors with potentially
683 central roles in specifying cell states.

684
685 We next employed TETRAMER, a tool integrating inferred differentiation states
686 during lineage progression with gene regulatory networks (GRNs) from publicly
687 available datasets (Cholley et al., 2018), for the reconstruction of GRNs whose
688 activity may define cell states within the oligodendroglial and neuronal lineages.
689 Briefly, lists of transcription factors expressed in the identified clusters of the
690 oligodendroglial and neuronal lineages as well as transcription factors that are
691 expressed in both of these lineages (“common” transcription factors), were used as
692 input by TETRAMER to explore gene expression profiles of mammalian tissues/cells
693 with comprehensive analysis of deposited ChIP-sequencing data corresponding to

694 transcription factor-binding and further comprising data on actively transcribed
695 enhancers and promoters. In the preliminary step, transcription factor-transcription
696 factor and transcription factor-target gene interactions were compiled for determining
697 regulatory interactions between shared neurogenesis- and oligodendrogenesis-
698 restricted (Figure S6b-c) transcription factors. A large proportion (89.3-91.8% of all
699 interactions) of transcription factor-target gene interactions for transcription factors
700 common to both lineages and those regulating neurogenesis consisted in predicted
701 target gene activation. Interestingly, however, activating and inhibiting regulatory
702 interactions were predicted to occur at similar frequencies between
703 oligodendrogenesis-specific transcription factors, highlighting qualitative differences
704 in how cell state transitions are controlled at the transcriptional level in the 2
705 lineages. Transcription factor interactions with target genes were quantified using the
706 Cytoscape network analysis parameters by probing the entire training GRN
707 reconstructed (as described in Figure 4) and presented as intensity heatmaps for the
708 top 25 transcription factors with the most global, activating and inhibiting target gene
709 interactions in Figure S6e (ranked transcription factor examples in Figure S6f).
710 Amongst the most highly ranked transcription factors were *Cebpa*, expressed in
711 OLqNSCII and best described in the context of myelopoiesis, where it inhibits
712 proliferation (see (Calella et al., 2007) for proposed roles during neural
713 development), and *Ezh2*, which promotes embryonic NSC proliferation and
714 differentiation into OPCs (Sher et al., 2008). Altogether, these analyses enable
715 ranking transcription factors that are likely to act as “master regulators” based on a
716 number of parameters that include their target gene regulation, protein-protein
717 interactions and diffusive effects downstream. To further investigate the major gene
718 regulatory cascades controlling adult oligodendrogenesis, the GRN assembled for

719 common transcription factors and oligodendrogenesis (Figure S6b,d) were combined
720 and merged with a recently assembled GRN for post-OPC stages of oligodendroglial
721 maturation (Cantone et al., 2019) (Figure 5), which defined the role of transcription
722 factors such as *Olig2*, *Sox10*, and *Tcf7l2* during oligodendrocyte differentiation and
723 maturation. Here, genes overlapping in later-stage oligodendrocytes from the
724 present study with those published recently (Cantone et al., 2019), were filtered and
725 represented as GO Biological Processes in a larger merged network (Figure 5).
726 Approximately, a quarter of the differentially expressed genes, as determined by the
727 Seurat analysis, were used in this TETRAMER analysis. Of note, modulation of
728 many of these genes has previously been reported during postnatal and adult
729 oligodendrogenesis from NSCs (Azim et al., 2015). This final network termed as
730 “AdultOLgenesis GRN” was used for further analysis as described below. The
731 individual stages were then positioned relative to the average positioning of single
732 cells/clusters in FateID pseudotime (Figure 1c) (see Materials and methods for
733 network assembly).

734

735 **Stage-specific GRN**

736 Focusing on target gene activation or repression in substages of the oligodendrocyte
737 lineage reveals varying and contrasting degrees of gene regulation (Figure 5a-f).
738 Notably, the OLqNSCII, OLaNSC and OLTAP stages exhibited prominent gene
739 regulatory activities, with OLaNSCs seemingly progressively activating TAP-specific
740 target genes (Figure 5b,e,f), whilst also inhibiting the expression of genes typical for
741 the most differentiated (OPC/mature oligodendrocyte) stages. This suggests that,
742 following activation, oligodendrocyte lineage cells would steadily progress to the TAP
743 stage, which could be temporarily stabilized by active repression of differentiation-

744 associated gene modules. Interestingly, the uniquely low expression levels of
745 transcription factors active in OLqNSCI and OLpNSCs are predicted to only modestly
746 result in GRN state restructuring at these stages. These findings demonstrate that
747 transcription factors expressed in distinct stages during oligodendrogenesis have
748 contrasting modes of gene regulation.

749

750 Next, the highest ranked transcription factors for each of the selected
751 oligodendrocyte lineage stages were probed for the extent to which their inferred
752 transcriptional regulatory activity propagates within the assembled GRN. The
753 downstream gene regulatory effects of *Olig2* and *Sox10*, which modulate the
754 expression of a large number of genes involved in gliogenic and neurogenic
755 processes (Cantone et al., 2019), provided a quantitative reference to assess the
756 GRN-modulating activity of newly identified transcription factors. The immediate
757 downstream target genes for *Olig2* and *Sox10* are presented in a subnetwork (Figure
758 5g), and downstream propagation cumulatively modulates 75% of all network
759 components within one further tier. The regulatory activity of *Mitf* and *Rreb1*,
760 expressed in OLqNSCI, spread the least within the GRN, supporting the previous
761 analysis (Figure S6e) that shows *Rreb1* as the highest ranked transcriptional
762 repressor (Figure 5h). The impact of OLqNSCII transcription factors *Cebpa* and
763 *Epas1* quantitatively resembles that of *Olig2* and *Sox10* (Figure 6i). Interestingly,
764 *Cebpa* has been described for myelopoiesis as inhibiting cell cycle-related genes
765 (Calella et al., 2007), which fits with its predicted inhibitory interactions with major
766 cell cycle genes expressed in TAPs, supporting its role as a quiescent NSC-specific
767 transcription factor. The 2 highest-ranked OLpNSC transcription factors, *Foxo1* and
768 *Nr1d1*, induce the expression of a number of cell cycle regulators expressed in

769 OLaNSCs and OLTAPs (Figure 5j). Like OLqNSCIIIs, OLaNSCs and OLTAPs
770 express transcription factors whose predicted influence on oligodendrocyte GRN
771 activity resembles that exerted by *Olig2* and *Sox10*. These findings identify putative
772 core regulators of stage-specific oligodendrocyte GRNs, thus complementing known
773 pan-oligodendrocyte transcription factors *Olig2* and *Sox10* and providing a view into
774 stage-specific control of oligodendroglial lineage progression.

775

776 **PANTHER Pathway Integration of GRNs**

777 Having defined GRN state transitions controlling oligodendrocyte lineage
778 progression, we attempted integrating this knowledge with stage-specific signaling
779 pathway activity predictions from our previous PANTHER analysis (Figure 2b),
780 reasoning that the identified signaling pathways would impact cell fate by ultimately
781 modulating transcriptional networks. We explored this hypothesis using the
782 reconstructed AdultOLgenesis GRN, examining signaling pathways known to
783 modulate at least 2 transcription factors expressed at a given stage, and then
784 assessing the predicted propagation of their transcriptional modulatory activity within
785 the GRN. The direct target genes and additional secondary target genes regulated
786 by both *Olig2* and *Sox10*, as performed in the prior analysis in Figure 5g, were used
787 as a gauge for transcriptional coverage of each tested transcription factor associated
788 with PANTHER pathway terms. In addition, the transcription factors induced by
789 selected PANTHER signaling pathways were ranked based on the number of
790 transcription factor-target gene interactions. These were further classified according
791 to their gene-activating, -inhibitory, and unspecified effects onto the oligodendrocyte
792 lineage in red, green, and grey, respectively (Figure 6a). In the earlier stages of the
793 oligodendrocyte lineage, Wnt signaling is predicted to affect approximately half as

794 many GRN components as those modulated by *Olig2* and *Sox10*. Our previous
795 reports demonstrated that manipulating the Wnt signaling pathway by pharmacologic
796 or genetic strategies increases the expression of *Ascl1*, *Olig2* and *Sox10* transcripts
797 by at least 2.5-fold (Azim, Fischer, et al., 2014; Azim, Rivera, et al., 2014). In the
798 present study, these essential transcription factors were indeed predicted to be
799 secondary target genes of the Wnt pathway (Figure 6a,b), thus potentially
800 accounting for the previously described enhancements of myelination following Wnt
801 signaling modulation (Azim et al., 2017; Azim, Fischer, et al., 2014; Azim, Rivera, et
802 al., 2014) and validating this strategy. PDGF signaling on the other hand induces
803 similar gene regulatory events as *Olig2* and *Sox10*, although initially repressing
804 genes expressed in later stage oligodendrocytes (Figure 6c), in line with its role as
805 an OPC mitogen. However, *Stat1* and *Stat5b*, transcription factors modulated by the
806 PDGF pathway, activate transcriptional networks in TAPs that enhance the
807 expression of genes in OPCs and mature oligodendrocytes, leading to extensive
808 downstream transcription factor induction that included a number of master
809 regulators (see heatmap in Figure 6c). Interestingly, the pathways active in
810 OLaNSCs (“Transcriptional regulation by bZIP transcription factors”, “Gonadotropin
811 signaling pathway”) and in OLTAPs (“General Transcriptional Regulation”) are
812 involved in a number of gene regulatory events larger even than those elicited by
813 *Olig2* and *Sox10*, suggesting extensive GRN reorganization at these stages,
814 possibly reflecting a lineage watershed on the way to differentiation. Indeed, a
815 number of the above identified master regulators (Figure S6e) are key effectors of
816 PANTHER pathway terms enriched in OLaNSCs and OLTAPs. Other potent
817 signaling pathways examined include Notch signaling and p53 active in OLaNSCs
818 (G1 and S phase) and TAPs (G2/M and S phase). Other pathways identified in the

819 earlier PANTHER analysis, including “Angiogenesis” (OLqNSCI), “Circadian clock”
820 (OLqNSCII/qNSCII) and “p53 Feedback Loops 2” (G2M and S phase
821 OLaNSC/OLTAP), had overall fewer predicted transcriptional effects. Altogether,
822 these findings demonstrate that large cohorts of transcription factors in the
823 reconstructed Core GRN are effectors of multiple signaling pathways and provide
824 useful insights into how environmental cues could affect transcriptional activities, and
825 thus lineage progression, during SVZ-derived oligodendrogenesis. Future studies will
826 aim at expanding these observations by testing the functionality of identified
827 signaling pathways and to confirm changes in target expression experimentally.

828 **Word count: 3500**

829

830 **DISCUSSION**

831 In the present study, a meta-analysis of single cell RNAseq data from the adult SVZ
832 was performed to resolve the transcriptional signatures that distinguish between
833 adult neurogenesis and oligodendrogenesis. Recent transcriptomic analyses
834 focusing on early postnatal development and adulthood (Azim et al., 2017; Azim et
835 al., 2015; Mizrak et al., 2019), provided some insights into the gene expression
836 profiles associated with oligodendrogenesis. A number of newer transcriptomics
837 studies of adult neurogenesis have shed light onto the molecular processes
838 regulating the generation of olfactory bulb neurons (reviewed in (Marcy & Raineteau,
839 2019)). In addition, landmark studies using single cell profiling of murine
840 oligodendrocytes from different stages of life in the CNS have immensely contributed
841 to our understanding of the heterogeneity and molecular regulation of
842 oligodendrocyte differentiation (Marques et al., 2018; Marques et al., 2016; Zeisel et
843 al., 2015). A recent elegant single-cell sequencing survey of the lateral and medial
844 walls of the young adult SVZ demonstrated that NSCs located in microdomains other
845 than the lateral wall generate oligodendrocytes (Mizrak et al., 2019), but an in-depth
846 investigation into the mechanisms controlling adult oligodendrogenesis had not yet
847 been performed. To this end, we analyzed recently generated single-cell data from
848 the SVZ (Basak et al., 2018) focusing on NSC/progenitor heterogeneity, in order to
849 identify putative oligodendrocyte- and neuron-restricted progenitors (Felipe Ortega et
850 al., 2013). Our findings reveal transcriptional regulators as major protein classes
851 modulating all stages of the SVZ-NSC-derived oligodendrocyte lineage.

852

853 We carefully inspected the transcriptomes of NSCs and TAPs for the expression of
854 known early oligodendroglial lineage marker genes (Figure S1). These included
855 members of the Sox transcription factor family and *Olig2/Olig1*, which were found to
856 be expressed selectively in NSC/TAPs that also expressed other known gliogenic
857 markers such as *Hopx*, *Notch* genes and their subsequent target genes of the *Hes*
858 family, overall resembling the pattern of expression observed during postnatal
859 oligodendrogenesis (Azim et al., 2015). Oligodendrocyte lineage NSCs/TAPs
860 amounted to approximately 7% of all NSCs and TAPs, which is in line with earlier
861 retroviral-fate mapping observations describing a similar oligodendrocyte/neuron
862 output ratio between from the adult SVZ (Menn et al., 2006). Comparison of single
863 cells at a defined stage of the two lineages showed only a modest degree of
864 separation in tSNE plots. While this implies close similarity between the early steps
865 of oligodendroglial and neuronal lineage progression, key differences were
866 associated with specific classes of genes, such as transcription factors. Notably,
867 more closely focusing on lineage-specific features by GO “Protein Class” and
868 “Pathway” analyses revealed that from the earliest quiescent NSC stages to TAPs,
869 the terms related to “transcriptional cues” accounted for most of the differences
870 between the two lineages. In agreement with the findings of the present study, these
871 broad classes of genes have recently been described as enriched in oligodendroglial
872 clusters of adult NSCs/TAPs (Mizrak et al., 2019), similar to observations made
873 during postnatal development in pre-OPC (TAPs) populations (Marques et al., 2018),
874 and elsewhere during embryonic oligodendrogenesis (Klum et al., 2018). Our
875 comprehensive side-by-side comparison of protein classes differentially expressed
876 by the two SVZ lineages unequivocally demonstrates transcriptional control as a
877 major determinant of fate specification and lineage progression and warranted

878 further in-depth characterization of the GRN controlling oligodendrogenesis (see
879 below). Pathway analysis of the most immature stages (qNSCI to TAP) in the two
880 lineages suggested previously unappreciated mechanisms controlling the generation
881 of adult oligodendrocytes from the SVZ. Important pathways detected in the qNSCI/II
882 and pNSC stages of the oligodendrocyte lineage included Wnt signaling,
883 angiogenesis and Notch signaling, all known as important pathways regulating adult
884 oligodendrogenesis (reviewed in (El Waly et al., 2014)). Other key pathway terms
885 derived from this analysis include “Circadian clock”, which has not previously been
886 described as a regulator of oligodendrogenesis, although an earlier study proposed
887 this pathway as a cell-intrinsic timer for inhibiting cell division in postnatal OPCs
888 (Gao, Durand, & Raff, 1997). Interestingly, PDGF signaling was uniquely enriched in
889 OLpNSCs in our analysis and we predict that this oligodendrocyte lineage stage
890 comprises the SVZ cell population previously reported to undergo *in vivo* expansion
891 upon exposure to infused PDGF-A (Jackson et al., 2006; Moore, Bain, Loh, &
892 Levison, 2014). Pathways detected in aNSC and TAP populations comprise “Cell
893 cycle”, “DNA/nucleotide synthesis” and “Transcriptional machineries”, consistent with
894 single cell profiling studies of adult neurogenesis (Dulken et al., 2019; Llorens-
895 Bobadilla et al., 2015). We also identified Notch signaling as a regulator of
896 oligodendrocyte-fated aNSCs and TAPs, which is in agreement with previous
897 observations in the context of early SVZ-derived gliomagenesis (Giachino et al.,
898 2015) and during OPC generation from embryonic NPCs (Cui et al., 2004).

899
900 Interestingly, scoring the early oligodendroglial and neuronal lineage cells for their
901 proliferative state revealed instead broad similarities between corresponding cell
902 stages, suggesting that lineage commitment and proliferative expansion are at least

903 in part independently controlled. These similarities were fewer at post-TAP stages,
904 where OPCs and the very earliest neuroblasts (before emigration via the rostral
905 migratory stream) comprised mostly of quiescent cells and proliferative states,
906 respectively. The latter stage, upon pharmacogenomically instructed manipulation for
907 directing specific cell fates in older adult mice, results in its expansion and
908 subsequent dorsal-SVZ-derived OPCs (Azim et al., 2017). In support of these
909 findings, “Nucleic acid binding” and “transcription factor” pathways were most
910 prominent during S phase compared to G1 and G2M phases, suggesting
911 transcriptional modulation associated with access to *de novo* synthesized DNA (e.g.
912 propagation or passive loss of modifications on newly added histones) (Figure 3e).
913 Thus, targeting transcription factor programs regulating cell cycle phases in adult
914 OL-TAPs as previously described (Azim et al., 2017), presents additional avenues in
915 promoting the generating of adult-born OPCs.

916

917 Establishment of a pan-oligodendrocyte GRN allowed us to investigate
918 transcriptional network organization during lineage progression, defining stage-
919 specific GRN states and their core regulators, which add to well-established broad-
920 oligodendrocyte transcription factors such as *Olig2* and *Sox10*. These transcription
921 factors are well-characterized as binding to the promoters of a large number of
922 genes regulating several aspects of NSC/progenitor behaviors. *Olig2*, aside from
923 regulating transcriptional programs associated with lineage progression and
924 myelination in the post-OPC stages, also represses proneuronal and quiescence
925 genes and activates genes that promote cell cycle entry and oligodendrogenesis in
926 NSCs/NPs (Mateo et al., 2015). A number of *Sox10* target genes overlap with those
927 of *Olig2* in later stage oligodendrocytes (Cantone et al., 2019), while comparatively

928 little is known about oligodendrocyte transcription factor genome occupancy patterns
929 in SVZ-NSCs. In our analysis, *Sox10* mRNA was detected already in OLaNSCs,
930 consistent with its expression downstream of *Olig2* (Liu et al., 2007) and we predict
931 *Sox10* to be downregulating genes expressed in the neuronal lineage, including *Sufu*
932 that represses signaling pathways (e.g. Wnt and Shh signaling) which limit the
933 specification of OPCs (Pozniak et al., 2010).

934

935 Surprisingly, transcriptional control of lineage progression was most marked during
936 the actively proliferating oligodendrocyte lineage stages (OLaNSC and OLTAP) and
937 at the OLqNSCII stage, which we explored for predictive functions of transcription
938 factors. In our reconstructed GRN, analyzing transcription factor-target gene
939 interactions in the oligodendrocyte lineage aside from the well-characterized
940 transcriptional regulators, we uncovered novel master regulators. We used our
941 reconstructed GRN for predicting gene regulatory functions of these putative master
942 regulators. Amongst those identified were *Cebpa*, which has been described to
943 regulate genes expressed in the cycling population of the oligodendrocyte lineage
944 (Calella et al., 2007), and *Mitf*, which activates the transcription of the *Dct* gene (Jiao
945 et al., 2006), previously identified as highly expressed in gliogenic SVZ-NSCs (Azim
946 et al., 2015). Transcription factors expressed by OLaNSCs tended to positively
947 regulate TAP-specific genes, thus possibly promoting rapid lineage progression,
948 while the set of TAP-expressed transcription factors suggests concomitant
949 reinforcement of the TAP-specific gene-expression program and repression of
950 differentiation-associated genes (Figure 6e,f). Indeed, target gene repression
951 emerged as more widespread than in the neuronal lineage and may reflect the need

952 for stabilization of an intermediate undifferentiated stage after initial lineage
953 progression and expansion downstream of NSCs (Menn et al., 2006).

954

955 Our work identified transcription factors/transcriptional networks in the earlier stages
956 of the oligodendrocyte lineage that had been poorly characterized, and future
957 mechanistic studies will aim to confirm their predicted gene regulatory control of
958 oligodendrogenesis. Finally, given the predicted relevance of environmental
959 signaling and transcriptional control over oligodendrocyte lineage progression, we
960 investigated the ability of extracellular signaling events to modulate core
961 transcriptional regulators of the oligodendrocyte GRN. Several well-established
962 signaling pathways were predicted to stage-specifically impinge on core GRN
963 components, suggesting a measure of environmental control over lineage
964 progression. Thus, while SVZ-derived oligodendrocyte lineages are capable of
965 remarkable intrinsic control over their maturation (F. Ortega et al., 2013), a series of
966 known and novel environmental factors can confer flexibility to this process by
967 regulating the expression of transcriptional modulators of oligodendrocyte lineage
968 progression.

969 **Word count: 1446**

970

971 **CONFLICTS OF INTEREST**

972 The authors have no competing or financial interests to declare.

973

974 **AUTHORS' CONTRIBUTIONS**

975 KA was responsible for the conceptualization, data curation, formal analysis, funding
976 acquisition, investigation, methodology, project administration, supervision. FC
977 contributed to writing, validation and data analysis. MC carried out data curation,
978 analysis, investigation validation, and methodology. RA contributed to writing, data
979 curation, formal analysis, investigation, methodology. JV was responsible for funding
980 acquisition, project administration, supervision; HPH: funding acquisition, supervision
981 and project administration. OB was involved in data curation, acquisition and
982 methodology. AB was responsible for writing, methodology, supervision and
983 validation. HPH was responsible for funding acquisition and project administration.
984 PK for funding acquisition, investigation, methodology, project administration,
985 supervision, validation and writing.

986

987 **OPEN RESEARCH**

988 Scripts developed for the first time, Cytoscape files, cluster specific gene lists, gene
989 matrices and any other raw data of this study are placed in the repository Github
990 <https://github.com/kasumaz/AdultOLgenesis>. Assistance for TETRAMER usage can
991 also be requested from Dr Marco A. Mendoza (mmendoza@genoscope.cns.fr). A
992 user friendly web interface that allows investigators to examine gene expression
993 across all single cells assembled will be made online upon acceptance with the

994 expertise of the lab of Julio Vera (see for example:

995 <https://www.curatopes.com/melanoma/>).

996

997 **REFERENCES**

998 Arion, D., Unger, T., Lewis, D. A., Levitt, P., & Mirnics, K. (2007). Molecular evidence
999 for increased expression of genes related to immune and chaperone function
1000 in the prefrontal cortex in schizophrenia. *Biol Psychiatry*, 62(7), 711-721. doi:
1001 10.1016/j.biopsych.2006.12.021

1002 Azim, K., Akkermann, R., Cantone, M., Vera, J., Jadasz, J. J., & Kury, P. (2018).
1003 Transcriptional Profiling of Ligand Expression in Cell Specific Populations of
1004 the Adult Mouse Forebrain That Regulates Neurogenesis. *Front Neurosci*, 12,
1005 220. doi: 10.3389/fnins.2018.00220

1006 Azim, K., Angonin, D., Marcy, G., Pieropan, F., Rivera, A., Donega, V., . . .
1007 Raineteau, O. (2017). Pharmacogenomic identification of small molecules for
1008 lineage specific manipulation of subventricular zone germinal activity. *PLoS
1009 Biol*, 15(3), e2000698. doi: 10.1371/journal.pbio.2000698

1010 Azim, K., Berninger, B., & Raineteau, O. (2016). Mosaic Subventricular Origins of
1011 Forebrain Oligodendrogenesis. *Front Neurosci*, 10, 107. doi:
1012 10.3389/fnins.2016.00107

1013 Azim, K., Fischer, B., Hurtado-Chong, A., Draganova, K., Cantu, C., Zemke, M., . . .
1014 Raineteau, O. (2014). Persistent Wnt/beta-catenin signaling determines
1015 dorsalization of the postnatal subventricular zone and neural stem cell
1016 specification into oligodendrocytes and glutamatergic neurons. *Stem Cells*,
1017 32(5), 1301-1312. doi: 10.1002/stem.1639

1018 Azim, K., Hurtado-Chong, A., Fischer, B., Kumar, N., Zweifel, S., Taylor, V., &
1019 Raineteau, O. (2015). Transcriptional Hallmarks of Heterogeneous Neural
1020 Stem Cell Niches of the Subventricular Zone. *Stem Cells*, 33(7), 2232-2242.
1021 doi: 10.1002/stem.2017

1022 Azim, K., Raineteau, O., & Butt, A. M. (2012). Intraventricular injection of FGF-2
1023 promotes generation of oligodendrocyte-lineage cells in the postnatal and
1024 adult forebrain. *GLIA*, 60(12), 1977-1990. doi: 10.1002/glia.22413

1025 Azim, K., Rivera, A., Raineteau, O., & Butt, A. M. (2014). GSK3beta regulates
1026 oligodendrogenesis in the dorsal microdomain of the subventricular zone via
1027 Wnt-beta-catenin signaling. *GLIA*, 62(5), 778-779. doi: 10.1002/glia.22641

1028 Basak, O., Krieger, T. G., Muraro, M. J., Wiebrands, K., Stange, D. E., Frias-
1029 Aldeguer, J., . . . Clevers, H. (2018). Troy+ brain stem cells cycle through
1030 quiescence and regulate their number by sensing niche occupancy. *Proc Natl
1031 Acad Sci U S A*, 115(4), E610-E619. doi: 10.1073/pnas.1715911114

1032 Butler, A., Hoffman, P., Smibert, P., Papalexi, E., & Satija, R. (2018). Integrating
1033 single-cell transcriptomic data across different conditions, technologies, and
1034 species. *Nat Biotechnol*, 36(5), 411-420. doi: 10.1038/nbt.4096

1035 Calella, A. M., Nerlov, C., Lopez, R. G., Sciarretta, C., von Bohlen und Halbach, O.,
1036 Bereshchenko, O., & Minichiello, L. (2007). Neurotrophin/Trk receptor
1037 signaling mediates C/EBPalpha, -beta and NeuroD recruitment to immediate-
1038 early gene promoters in neuronal cells and requires C/EBPs to induce
1039 immediate-early gene transcription. *Neural Dev*, 2, 4. doi: 10.1186/1749-8104-
1040 2-4

1041 Calzolari, F., Michel, J., Baumgart, E. V., Theis, F., Gotz, M., & Ninkovic, J. (2015).
1042 Fast clonal expansion and limited neural stem cell self-renewal in the adult
1043 subependymal zone. *Nat Neurosci*, 18(4), 490-492. doi: 10.1038/nn.3963

1044 Cantone, M., Kuspert, M., Reiprich, S., Lai, X., Eberhardt, M., Gottle, P., . . . Vera, J.
1045 (2019). A gene regulatory architecture that controls region-independent
1046 dynamics of oligodendrocyte differentiation. *GLIA*. doi: 10.1002/glia.23569

1047 Capilla-Gonzalez, V., Cebrian-Silla, A., Guerrero-Cazares, H., Garcia-Verdugo, J.
1048 M., & Quinones-Hinojosa, A. (2013). The generation of oligodendroglial cells
1049 is preserved in the rostral migratory stream during aging. *Front Cell Neurosci*,
1050 7, 147. doi: 10.3389/fncel.2013.00147

1051 Carlin, D. E., Demchak, B., Pratt, D., Sage, E., & Ideker, T. (2017). Network
1052 propagation in the cytoscape cyberinfrastructure. *PLoS Comput Biol*, 13(10),
1053 e1005598. doi: 10.1371/journal.pcbi.1005598

1054 Chen, J., Van Gulden, S., McGuire, T. L., Fleming, A. C., Oka, C., Kessler, J. A., &
1055 Peng, C. Y. (2018). BMP-Responsive Protease HtrA1 Is Differentially
1056 Expressed in Astrocytes and Regulates Astrocytic Development and Injury
1057 Response. *J Neurosci*, 38(15), 3840-3857. doi: 10.1523/JNEUROSCI.2031-
1058 17.2018

1059 Cholley, P. E., Moehlin, J., Rohmer, A., Zilliox, V., Nicaise, S., Gronemeyer, H., &
1060 Mendoza-Parra, M. A. (2018). Modeling gene-regulatory networks to describe
1061 cell fate transitions and predict master regulators. *NPJ Syst Biol Appl*, 4, 29.
1062 doi: 10.1038/s41540-018-0066-z

1063 Crawford, A. H., Tripathi, R. B., Richardson, W. D., & Franklin, R. J. (2016).
1064 Developmental Origin of Oligodendrocyte Lineage Cells Determines
1065 Response to Demyelination and Susceptibility to Age-Associated Functional
1066 Decline. *Cell Rep*. doi: 10.1016/j.celrep.2016.03.069

1067 Cui, X. Y., Hu, Q. D., Tekaya, M., Shimoda, Y., Ang, B. T., Nie, D. Y., . . . Xiao, Z. C.
1068 (2004). NB-3/Notch1 pathway via Deltex1 promotes neural progenitor cell
1069 differentiation into oligodendrocytes. *J Biol Chem*, 279(24), 25858-25865. doi:
1070 10.1074/jbc.M313505200

1071 Dulken, B. W., Buckley, M. T., Navarro Negredo, P., Saligrama, N., Cayrol, R.,
1072 Leeman, D. S., . . . Brunet, A. (2019). Single-cell analysis reveals T cell
1073 infiltration in old neurogenic niches. *Nature*, 571(7764), 205-210. doi:
1074 10.1038/s41586-019-1362-5

1075 Dulken, B. W., Leeman, D. S., Boutet, S. C., Hebestreit, K., & Brunet, A. (2017).
1076 Single-Cell Transcriptomic Analysis Defines Heterogeneity and
1077 Transcriptional Dynamics in the Adult Neural Stem Cell Lineage. *Cell Rep*,
1078 18(3), 777-790. doi: 10.1016/j.celrep.2016.12.060

1079 Durinck, S., Spellman, P. T., Birney, E., & Huber, W. (2009). Mapping identifiers for
1080 the integration of genomic datasets with the R/Bioconductor package
1081 biomaRt. *Nat Protoc*, 4(8), 1184-1191. doi: 10.1038/nprot.2009.97

1082 El Waly, B., Macchi, M., Cayre, M., & Durbec, P. (2014). Oligodendrogenesis in the
1083 normal and pathological central nervous system. *Front Neurosci*, 8, 145. doi:
1084 10.3389/fnins.2014.00145

1085 Figueres-Onate, M., Sanchez-Villalon, M., Sanchez-Gonzalez, R., & Lopez-
1086 Mascaraque, L. (2019). Lineage Tracing and Cell Potential of Postnatal Single
1087 Progenitor Cells In Vivo. *Stem Cell Reports*, 13(4), 700-712. doi:
1088 10.1016/j.stemcr.2019.08.010

1089 Fiorelli, R., Azim, K., Fischer, B., & Raineteau, O. (2015). Adding a spatial dimension
1090 to postnatal ventricular-subventricular zone neurogenesis. *Development*,
1091 142(12), 2109-2120. doi: 10.1242/dev.119966

1092 Franz, M., Rodriguez, H., Lopes, C., Zuberi, K., Montojo, J., Bader, G. D., & Morris,
1093 Q. (2018). GeneMANIA update 2018. *Nucleic Acids Res*, 46(W1), W60-W64.
1094 doi: 10.1093/nar/gky311

1095 Fuentealba, L. C., Rompani, S. B., Parraguez, J. I., Obernier, K., Romero, R.,
1096 Cepko, C. L., & Alvarez-Buylla, A. (2015). Embryonic Origin of Postnatal
1097 Neural Stem Cells. *Cell*, 161(7), 1644-1655. doi: 10.1016/j.cell.2015.05.041

1098 Gao, F. B., Durand, B., & Raff, M. (1997). Oligodendrocyte precursor cells count time
1099 but not cell divisions before differentiation. *Curr Biol*, 7(2), 152-155. doi:
1100 10.1016/s0960-9822(06)00060-1

1101 Giachino, C., Boulay, J. L., Ivanek, R., Alvarado, A., Tostado, C., Lugert, S., . . .
1102 Taylor, V. (2015). A Tumor Suppressor Function for Notch Signaling in
1103 Forebrain Tumor Subtypes. *Cancer Cell*, 28(6), 730-742. doi:
1104 10.1016/j.ccr.2015.10.008

1105 Grun, D., Lyubimova, A., Kester, L., Wiebrands, K., Basak, O., Sasaki, N., . . . van
1106 Oudenaarden, A. (2015). Single-cell messenger RNA sequencing reveals rare
1107 intestinal cell types. *Nature*, 525(7568), 251-255. doi: 10.1038/nature14966

1108 He, D., Marie, C., Zhao, C., Kim, B., Wang, J., Deng, Y., . . . Lu, Q. R. (2016). Chd7
1109 cooperates with Sox10 and regulates the onset of CNS myelination and
1110 remyelination. *Nat Neurosci*, 19(5), 678-689. doi: 10.1038/nn.4258

1111 Herman, J. S., Sagar, & Grun, D. (2018). FateID infers cell fate bias in multipotent
1112 progenitors from single-cell RNA-seq data. *Nat Methods*, 15(5), 379-386. doi:
1113 10.1038/nmeth.4662

1114 Jackson, E. L., Garcia-Verdugo, J. M., Gil-Perotin, S., Roy, M., Quinones-Hinojosa,
1115 A., VandenBerg, S., & Alvarez-Buylla, A. (2006). PDGFR alpha-positive B
1116 cells are neural stem cells in the adult SVZ that form glioma-like growths in
1117 response to increased PDGF signaling. *Neuron*, 51(2), 187-199. doi:
1118 10.1016/j.neuron.2006.06.012

1119 Jain, R., Li, D., Gupta, M., Manderfield, L. J., Ifkovits, J. L., Wang, Q., . . . Epstein, J.
1120 A. (2015). HEART DEVELOPMENT. Integration of Bmp and Wnt signaling by
1121 Hopx specifies commitment of cardiomyoblasts. *Science*, 348(6242),
1122 aaa6071. doi: 10.1126/science.aaa6071

1123 Jebb, D., & Hiller, M. (2018). Recurrent loss of HMGCS2 shows that ketogenesis is
1124 not essential for the evolution of large mammalian brains. *Elife*, 7. doi:
1125 10.7554/eLife.38906

1126 Jiao, Z., Zhang, Z. G., Hornyak, T. J., Hozeska, A., Zhang, R. L., Wang, Y., . . .
1127 Chopp, M. (2006). Dopachrome tautomerase (Dct) regulates neural progenitor
1128 cell proliferation. *Dev Biol*, 296(2), 396-408. doi: 10.1016/j.ydbio.2006.06.006

1129 Kessaris, N., Fogarty, M., Iannarelli, P., Grist, M., Wegner, M., & Richardson, W. D.
1130 (2006). Competing waves of oligodendrocytes in the forebrain and postnatal
1131 elimination of an embryonic lineage. *Nat Neurosci*, 9(2), 173-179. doi:
1132 10.1038/nn1620

1133 Kim, D. Y., Hwang, I., Muller, F. L., & Paik, J. H. (2015). Functional regulation of
1134 FoxO1 in neural stem cell differentiation. *Cell Death Differ*, 22(12), 2034-2045.
1135 doi: 10.1038/cdd.2015.123

1136 Klum, S., Zaouter, C., Alekseenko, Z., Bjorklund, A. K., Hagey, D. W., Ericson, J., . . .
1137 Bergsland, M. (2018). Sequentially acting SOX proteins orchestrate
1138 astrocyte- and oligodendrocyte-specific gene expression. *EMBO Rep*, 19(11).
1139 doi: 10.15252/embr.201846635

1140 Liu, Z., Hu, X., Cai, J., Liu, B., Peng, X., Wegner, M., & Qiu, M. (2007). Induction of
1141 oligodendrocyte differentiation by Olig2 and Sox10: evidence for reciprocal

1142 interactions and dosage-dependent mechanisms. *Dev Biol*, 302(2), 683-693.
1143 doi: 10.1016/j.ydbio.2006.10.007

1144 Llorens-Bobadilla, E., Zhao, S., Baser, A., Saiz-Castro, G., Zwadlo, K., & Martin-
1145 Villalba, A. (2015). Single-Cell Transcriptomics Reveals a Population of
1146 Dormant Neural Stem Cells that Become Activated upon Brain Injury. *Cell*
1147 *Stem Cell*, 17(3), 329-340. doi: 10.1016/j.stem.2015.07.002

1148 Lukaszewicz, A. I., & Anderson, D. J. (2011). Cyclin D1 promotes neurogenesis in
1149 the developing spinal cord in a cell cycle-independent manner. *Proc Natl Acad*
1150 *Sci U S A*, 108(28), 11632-11637. doi: 10.1073/pnas.1106230108

1151 Marcy, G., & Raineteau, O. (2019). Concise Review: Contributions of single cell
1152 approaches for probing heterogeneity and dynamics of neural progenitors
1153 throughout life. *Stem Cells*. doi: 10.1002/stem.3071

1154 Marques, S., van Bruggen, D., Vanichkina, D. P., Floriddia, E. M., Munguba, H.,
1155 Varemo, L., . . . Castelo-Branco, G. (2018). Transcriptional Convergence of
1156 Oligodendrocyte Lineage Progenitors during Development. *Dev Cell*, 46(4),
1157 504-517 e507. doi: 10.1016/j.devcel.2018.07.005

1158 Marques, S., Zeisel, A., Codeluppi, S., van Bruggen, D., Mendanha Falcao, A., Xiao,
1159 L., . . . Castelo-Branco, G. (2016). Oligodendrocyte heterogeneity in the
1160 mouse juvenile and adult central nervous system. *Science*, 352(6291), 1326-
1161 1329. doi: 10.1126/science.aaf6463

1162 Mateo, J. L., van den Berg, D. L., Haeussler, M., Drechsel, D., Gaber, Z. B., Castro,
1163 D. S., . . . Martynoga, B. (2015). Characterization of the neural stem cell gene
1164 regulatory network identifies OLIG2 as a multifunctional regulator of self-
1165 renewal. *Genome Res*, 25(1), 41-56. doi: 10.1101/gr.173435.114

1166 Menn, B., Garcia-Verdugo, J. M., Yaschine, C., Gonzalez-Perez, O., Rowitch, D., &
1167 Alvarez-Buylla, A. (2006). Origin of oligodendrocytes in the subventricular
1168 zone of the adult brain. *The Journal of neuroscience : the official journal of the*
1169 *Society for Neuroscience*, 26(30), 7907-7918.

1170 Merkle, F. T., Fuentealba, L. C., Sanders, T. A., Magno, L., Kessaris, N., & Alvarez-
1171 Buylla, A. (2014). Adult neural stem cells in distinct microdomains generate
1172 previously unknown interneuron types. *Nat Neurosci*, 17(2), 207-214. doi:
1173 10.1038/nn.3610

1174 Merkle, F. T., Mirzadeh, Z., & Alvarez-Buylla, A. (2007). Mosaic organization of
1175 neural stem cells in the adult brain. *Science*, 317(5836), 381-384.

1176 Mi, H., Poudel, S., Muruganujan, A., Casagrande, J. T., & Thomas, P. D. (2016).
1177 PANTHER version 10: expanded protein families and functions, and analysis
1178 tools. *Nucleic Acids Res*, 44(D1), D336-342. doi: 10.1093/nar/gkv1194

1179 Mirzadeh, Z., Doetsch, F., Sawamoto, K., Wichterle, H., & Alvarez-Buylla, A. (2010).
1180 The subventricular zone en-face: wholemount staining and ependymal flow. *J*
1181 *Vis Exp*(39). doi: 10.3791/1938

1182 Mizrak, D., Levitin, H. M., Delgado, A. C., Crotet, V., Yuan, J., Chaker, Z., . . .
1183 Doetsch, F. (2019). Single-Cell Analysis of Regional Differences in Adult V-
1184 SVZ Neural Stem Cell Lineages. *Cell Rep*, 26(2), 394-406 e395. doi:
1185 10.1016/j.celrep.2018.12.044

1186 Moore, L., Bain, J. M., Loh, J. M., & Levison, S. W. (2014). PDGF-responsive
1187 progenitors persist in the subventricular zone across the lifespan. *ASN Neuro*,
1188 6(2). doi: 10.1042/AN20120041

1189 Nakatani, H., Martin, E., Hassani, H., Clavairoly, A., Maire, C. L., Viadieu, A., . . .
1190 Parras, C. (2013). Ascl1/Mash1 promotes brain oligodendrogenesis during

1191 myelination and remyelination. *J Neurosci*, 33(23), 9752-9768. doi:
1192 10.1523/JNEUROSCI.0805-13.2013

1193 Obernier, K., Cebrian-Silla, A., Thomson, M., Parraguez, J. I., Anderson, R., Guinto,
1194 C., . . . Alvarez-Buylla, A. (2018). Adult Neurogenesis Is Sustained by
1195 Symmetric Self-Renewal and Differentiation. *Cell Stem Cell*, 22(2), 221-234
1196 e228. doi: 10.1016/j.stem.2018.01.003

1197 Oki, S., Ohta, T., Shioi, G., Hatanaka, H., Ogasawara, O., Okuda, Y., . . . Meno, C.
1198 (2018). ChIP-Atlas: a data-mining suite powered by full integration of public
1199 ChIP-seq data. *EMBO Rep*, 19(12). doi: 10.15252/embr.201846255

1200 Ortega, F., Gascon, S., Masserdotti, G., Deshpande, A., Simon, C., Fischer, J., . . .
1201 Berninger, B. (2013). Oligodendroglionic and neurogenic adult
1202 subependymal zone neural stem cells constitute distinct lineages and exhibit
1203 differential responsiveness to Wnt signalling. *Nat Cell Biol*, 15(6), 602-613.
1204 doi: 10.1038/ncb2736

1205 Ortega, F., Gascón, S., Masserdotti, G., Deshpande, A., Simon, C., Fischer, J., . . .
1206 Berninger, B. (2013). Oligodendroglionic and neurogenic adult
1207 subependymal zone neural stem cells constitute distinct lineages and exhibit
1208 differential responsiveness to Wnt signalling. *Nat Cell Biol*, 15(6), 602-613.
1209 doi: 10.1038/ncb2736

1210 Poth, J. M., Brodsky, K., Ehrentraut, H., Grenz, A., & Eltzschig, H. K. (2013).
1211 Transcriptional control of adenosine signaling by hypoxia-inducible
1212 transcription factors during ischemic or inflammatory disease. *J Mol Med
(Berl)*, 91(2), 183-193. doi: 10.1007/s00109-012-0988-7

1213 Pozniak, C. D., Langseth, A. J., Dijkgraaf, G. J., Choe, Y., Werb, Z., & Pleasure, S.
1214 J. (2010). Sox10 directs neural stem cells toward the oligodendrocyte lineage
1215 by decreasing Suppressor of Fused expression. *Proc Natl Acad Sci U S A*,
1216 107(50), 21795-21800. doi: 10.1073/pnas.1016485107

1217 Rosmaninho, P., Mukusch, S., Piscopo, V., Teixeira, V., Raposo, A. A., Warta, R., . . .
1218 Castro, D. S. (2018). Zeb1 potentiates genome-wide gene transcription with
1219 Lef1 to promote glioblastoma cell invasion. *Embo J*, 37(15). doi:
1220 10.1525/embj.201797115

1221 Sher, F., Rossler, R., Brouwer, N., Balasubramaniyan, V., Boddeke, E., & Copray, S.
1222 (2008). Differentiation of neural stem cells into oligodendrocytes: involvement
1223 of the polycomb group protein Ezh2. *Stem Cells*, 26(11), 2875-2883. doi:
1224 10.1634/stemcells.2008-0121

1225 Simion, C., Cedano-Prieto, M. E., & Sweeney, C. (2014). The LRIG family: enigmatic
1226 regulators of growth factor receptor signaling. *Endocr Relat Cancer*, 21(6),
1227 R431-443. doi: 10.1530/ERC-14-0179

1228 Zeisel, A., Munoz-Manchado, A. B., Codeluppi, S., Lonnerberg, P., La Manno, G.,
1229 Jureus, A., . . . Linnarsson, S. (2015). Brain structure. Cell types in the mouse
1230 cortex and hippocampus revealed by single-cell RNA-seq. *Science*,
1231 347(6226), 1138-1142. doi: 10.1126/science.aaa1934

1232 Zweifel, S., Marcy, G., Lo Guidice, Q., Li, D., Heinrich, C., Azim, K., & Raineteau, O.
1233 (2018). HOPX Defines Heterogeneity of Postnatal Subventricular Zone Neural
1234 Stem Cells. *Stem Cell Reports*, 11(3), 770-783. doi:
1235 10.1016/j.stemcr.2018.08.006

1236

1237

1238 **References Word Count: 2244**

1239

1240 **FIGURE LEGENDS**

1241 **Figure 1**

1242 Identification of lineage-specific NSCs/NPs. (a) tSNE plot of 1200 single cells
1243 (including microglia, choroid plexus, neurons and vascular cells; see Figure S1)
1244 expressing the transcription factors *Olig1*, *Olig2* and *Sox10*. PCA color plot of
1245 transcript expression for determining cells with elevated expression of core
1246 oligodendrocyte lineage markers. (b) Selected early oligodendrocyte lineage cell
1247 expression of pallial marker *Pax6* and subpallial markers *Nkx2.1* and *Gsx2* together
1248 with the NSC marker *Hes5* for determining a potential dorsal origin of
1249 oligodendrocyte lineage. (c) FateID pseudotime demonstrates that the mature
1250 oligodendrocyte (MOL) transcriptional trajectory branches off only at the very earliest
1251 stages in the neuronal lineage, whereas among identified oligodendrocyte cells
1252 mature oligodendrocytes branch via OPCs that are in close proximity to OLTAPs and
1253 OLaNSCs. (d) tSNE plots of proneuronal and proolidendroglial lineage cells and
1254 selected transcript expression in the early- and mid-stages of the oligodendrocyte
1255 lineage. e Heatmap of the 13 analyzed clusters illustrating the highly enriched stage-
1256 specific signatures. Stage color legend is presented in f. (f) Violin plots of selected
1257 marker expression across the 13 clusters further demonstrating markers
1258 specific/enriched in stage and lineage. Abbreviations: aNSC: activated neural stem
1259 cell; MOL: mature oligodendrocyte; NB: neuroblast; NSC: neural stem cell; OLaNSC:
1260 oligodendroglial activated neural stem cell; OLpNSC: oligodendroglial primed neural
1261 stem cell; OLqNSCI: oligodendroglial quiescent neural stem cell (subtype I);
1262 OLqNSCI: oligodendroglial quiescent neural stem cell (subtype II); OLTAP:

1263 oligodendroglial transiently amplifying progenitor; OPC: oligodendrocyte precursor
1264 cell; pNSC: primed neural stem cell; qNSCI: quiescent neural stem cell (subtype I);
1265 qNSCII: quiescent neural stem cell (subtype II).

1266

1267 **Figure 2**

1268 Pathway and mechanistic analysis of the oligodendrocyte lineage. (a) Dot plot of the
1269 most highly enriched/significant (“Sig” in plot) signaling pathways, organized
1270 alphabetically from top to bottom in the 2 lineages. (b) A time course of the top 5
1271 most enriched biological processes in each of the 7 clusters in the oligodendrocyte
1272 lineage. Point size in plots reflects significance. Sig = significance (p -value).
1273 Abbreviations: aNSC: activated neural stem cell; MOL: mature oligodendrocyte; NB:
1274 neuroblast; NSC: neural stem cell; OPC: oligodendrocyte precursor cell; pNSC:
1275 primed neural stem cell; qNSCI: quiescent neural stem cell (subtype I); qNSCII:
1276 quiescent neural stem cell (subtype II).

1277

1278

1279 **Figure 3**

1280 Cell cycle heterogeneity of oligodendroglial and neuronal lineage cells. (a)
1281 Oligodendrocyte and neuronal lineage cells scored by Seurat for cell cycle
1282 regression using canonical markers. Oligodendrocyte lineage cells are plotted
1283 according to their pseudotime trajectory and overlaid displayed the phase of cycle of
1284 each cell. (b) A summary displaying the percentage of cells in the 3 phases of cell
1285 cycle and the dynamics of mid stages of either lineage shuttling between states. (c)
1286 Ridge plot of oligodendrocyte and neuronal lineage cells illustrating the distribution of
1287 signal in the S or G2M cell cycle phase. (d) The mid stages of oligodendroglial (light

1288 red) and neuronal lineage (light blue) expanded for S (*Pcna*, *Mcm6*) and G2M
1289 (*Top2a*, *Mki67*) marker signal distribution in ridge plots. (e,f) Dot plots show pathway
1290 and protein class identification of the mid stages in the oligodendrocyte lineage.
1291 Green, light red and brown in OLaNSC labels quiescent, common to both stages and
1292 S phase, respectively; light purple, light red and light brown label OLTAPs in G2M,
1293 common to both and S phase, respectively. Terms are ranked according to their
1294 highest significance (Sig; *p*-value) from top to bottom. Pathways in red font are
1295 examined for revealing their signaling-to-transcriptional networks in Figure 7.
1296 Abbreviations: aNSC: activated neural stem cell; MOL: mature oligodendrocyte; NB:
1297 neuroblast; NSC: neural stem cell; OLaNSC: oligodendroglial activated neural stem
1298 cell; OLpNSC: oligodendroglial primed neural stem cell; OLqNSCI: oligodendroglial
1299 quiescent neural stem cell (subtype I); OLqNSCI: oligodendroglial quiescent neural
1300 stem cell (subtype II); OLTAP: oligodendroglial transiently amplifying progenitor;
1301 OPC: oligodendrocyte precursor cell; pNSC: primed neural stem cell; qNSCI:
1302 quiescent neural stem cell (subtype I); qNSCII: quiescent neural stem cell (subtype);
1303 TF: transcription factor.

1304

1305 **Figure 4**

1306 Reconstruction of a GRN by merging of previously generated networks and
1307 organization of stages in the oligodendrocyte lineage according to their pseudotime
1308 coordinates. Networks assembled in Figure S6b and d, those published recently (see
1309 description in results section) and additional transcription factor-target gene (TG)
1310 interactions from CHIP-seq studies are processed for a larger network. transcription
1311 factor expressed in 7 distinct stages are arranged according to their pseudotime
1312 order and each node represents the relative numbers of transcription factors

1313 expressed in a given phase in the lineage. A separate grouping of transcription
1314 factors expressed in both aNSCs and TAPs are plotted according to the average
1315 trajectory coordinates between these 2 phases. The top 5 GO Biological Processes
1316 in OPCs and mature oligodendrocytes are incorporated for identifying their
1317 regulatory pathways. Irregularly expressed transcription factors are those which are
1318 abundant in the neuronal lineage and additionally expressed along the
1319 oligodendrocyte lineage. The entire GRN of the oligodendrocyte lineage, termed as
1320 “AdultOLgenesis GRN”. Nodes in bold outer surface are characterized by high
1321 protein-protein interactions. Green, red and grey interactions signify gene inhibition,
1322 activation and unspecified interaction onto their target genes (TGs), respectively.
1323 Legends for the AdultOLgenesis GRN are presented in Figure 5 and 6.
1324 Abbreviations: aNSC: activated neural stem cell; GRN: gene regulatory network;
1325 MOL: mature oligodendrocyte; NB: neuroblast; NSC: neural stem cell; OLaNSC:
1326 oligodendroglial activated neural stem cell; OLpNSC: oligodendroglial primed neural
1327 stem cell; OLqNSCI: oligodendroglial quiescent neural stem cell (subtype I);
1328 OLqNSCI: oligodendroglial quiescent neural stem cell (subtype II); OLTAP:
1329 oligodendroglial transiently amplifying progenitor; OPC: oligodendrocyte precursor
1330 cell; TF: transcription factor; TG: target gene.

1331

1332 **Figure 5**

1333 Gene regulatory interactions in substages of the oligodendrocyte lineage and the
1334 predicted effects of key transcription factors in each stage. (a-f) Summaries of the
1335 GRNs in each stage showing downstream gene regulation propagation. Edges and
1336 nodes reflect the relative numbers of gene regulatory interactions and numbers of
1337 transcription factor expressed in each stage, respectively. (g-l) The downstream

1338 gene regulatory interactions of selected transcription factors are quantified by
1339 propagating the transcription factor most highly ranked in the oligodendrocyte
1340 lineage and a transcription factor that is commonly expressed in a defined stage. In
1341 g, *Olig2* and *Sox10* are probed for their downstream target (designated as
1342 secondary, 2°), the subsequent downstream targets (including both genes in the GO
1343 Biological Processes and additional transcription factors) to the tertiary genes (3°).
1344 The transcription factor-target interactions quantified are plotted as a percentage
1345 versus the total numbers of genes/gene regulatory interactions from the entire
1346 reconstructed GRN. For each stage, the 2 highly ranked transcription factors and
1347 their direct target genes are shown as subnetworks from the entire GRN.
1348 Abbreviations: aNSC: activated neural stem cell; GRN: gene regulatory network;
1349 MOL: mature oligodendrocyte; NB: neuroblast; NSC: neural stem cell; OLaNSC:
1350 oligodendroglial activated neural stem cell; OLpNSC: oligodendroglial primed neural
1351 stem cell; OLqNSCI: oligodendroglial quiescent neural stem cell (subtype I);
1352 OLqNSCI: oligodendroglial quiescent neural stem cell (subtype II); OLTAP:
1353 oligodendroglial transiently amplifying progenitor; OPC: oligodendrocyte precursor
1354 cell; TF: transcription factor; TG: target gene.

1355

1356 **Figure 6**

1357 Mapping the impact of Signaling/PANTHER pathways onto GRNs. (a) PANTHER
1358 pathways from previous GO analyses were used to filter out transcription factors
1359 associated with each pathway term and their propagation onto the GRN were
1360 quantified and represented as a percentage compared to *Olig2/Sox10* (Figure 5g).
1361 (b-g) Examples of PANTHER Pathway effects onto the reconstructed GRN where
1362 dashed edges show the secondary effects of propagation compared to the direct

1363 effects of transcription factors associated with each pathway. Heatmaps show the
1364 relative ranking of key transcription factors of each pathway (both direct and
1365 secondary targets). Transcription factors highlighted in red, green and grey are those
1366 that activate expression of genes in later stage oligodendrocytes, inhibit the
1367 expression of genes in later stage oligodendrocytes and transcription factors that are
1368 essential to pathways as general regulators, respectively. Abbreviations: aNSC:
1369 activated neural stem cell; GRN: gene regulatory network; MOL: mature
1370 oligodendrocyte; NB: neuroblast; NSC: neural stem cell; OLaNSC: oligodendroglial
1371 activated neural stem cell; OLpNSC: oligodendroglial primed neural stem cell;
1372 OLqNSCI: oligodendroglial quiescent neural stem cell (subtype I); OLqNSCI:
1373 oligodendroglial quiescent neural stem cell (subtype II); OLTAP: oligodendroglial
1374 transiently amplifying progenitor; OPC: oligodendrocyte precursor cell; TF:
1375 transcription factor; TG: target gene.

1376 **Word Count: 1333**

1377

1378 **Funding**

1379 This work was supported by the German Research Council (DFG;
1380 SPP1757/KU1934/2_1, KU1934/5-1; AZ/115/1-1/Ve642/1-1), the German Academic
1381 Exchange Service (DAAD), the Swiss National Funds (P300PA_171224). PK: This
1382 study was supported by the Deutsche Forschungsgemeinschaft (DFG; AZ115/1-1).
1383 Research on myelin repair and neuroregeneration has also been supported by the
1384 Christiane and Claudia Hempel Foundation for clinical stem cell research, DMSG
1385 Ortsvereinigung Düsseldorf und Umgebung e.V., Stifterverband/Novartisstiftung and
1386 the James and Elisabeth Cloppenburg, Peek & Cloppenburg Düsseldorf Stiftung.

1387 The MS Center at the Department of Neurology is supported in part by the Walter
1388 and Ilse Rose Foundation. FC was supported in part by NEURON-ERANET
1389 (01EW1604) and DFG (CRC1080) awards to Prof Benedikt Berninger (UMC Mainz)
1390 and by the Inneruniversitäre Forschungsförderung of the University Medical Center
1391 of Johannes Gutenberg University Mainz. AB was supported by grants from the MS
1392 Society UK, BBSRC and MRC.

1393 **List of abbreviations**

1394 aNSC: activated neural stem cell; CNS: central nervous system; DEGs: differentially
1395 expressed genes; GO: gene ontology GRN: gene regulatory network; MOL: mature
1396 oligodendrocyte; NB: neuroblast; NSC: neural stem cell; oligodendrocyte:
1397 oligodendrocyte; OLaNSC: oligodendroglial activated neural stem cell; OLpNSC:
1398 oligodendroglial primed neural stem cell; OLqNSCI: oligodendroglial quiescent
1399 neural stem cell (subtype I); OLqNSCI: oligodendroglial quiescent neural stem cell
1400 (subtype II); OLTAp: oligodendroglial transiently amplifying progenitor; OPC:
1401 oligodendrocyte precursor cell; PANTHER: protein annotation through evolutionary
1402 relationship; PCA: principal component analysis; pNSC: primed neural stem cell;
1403 qNSCI: quiescent neural stem cell (subtype I); qNSCII: quiescent neural stem cell
1404 (subtype II); SVZ: subventricular zone; TAP: transiently amplifying progenitor;
1405 TETRAMER: TEmporal TRAnscription regulation ModellER TF: transcription factor;
1406 TG: target gene; tSNE: t-Distributed Stochastic Neighbor Embedding.

1407

Figure 1: Identification of lineage-specific NSCs/NPs.

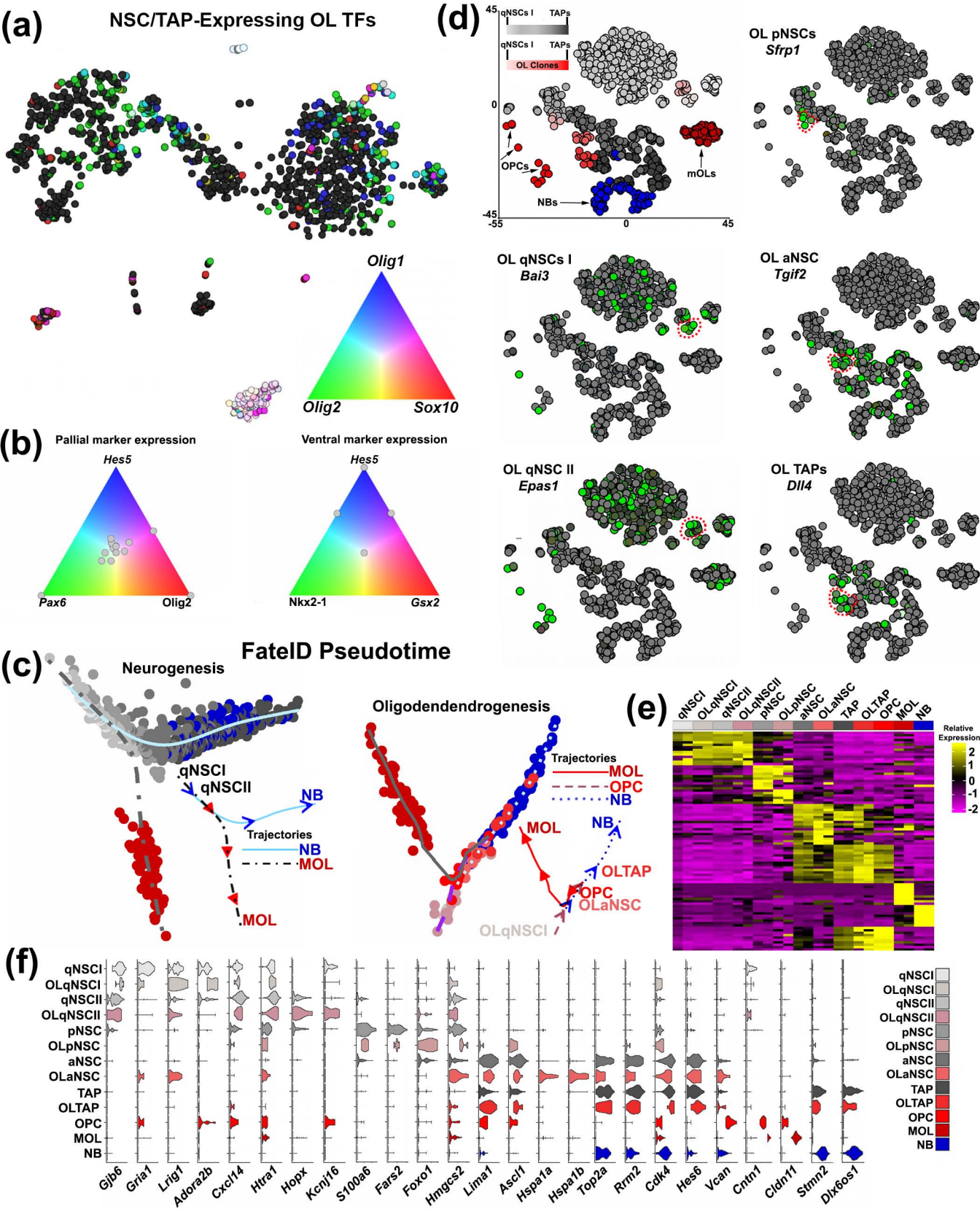


Figure 2: Pathway and mechanistic analysis of the oligodendrocyte lineage.

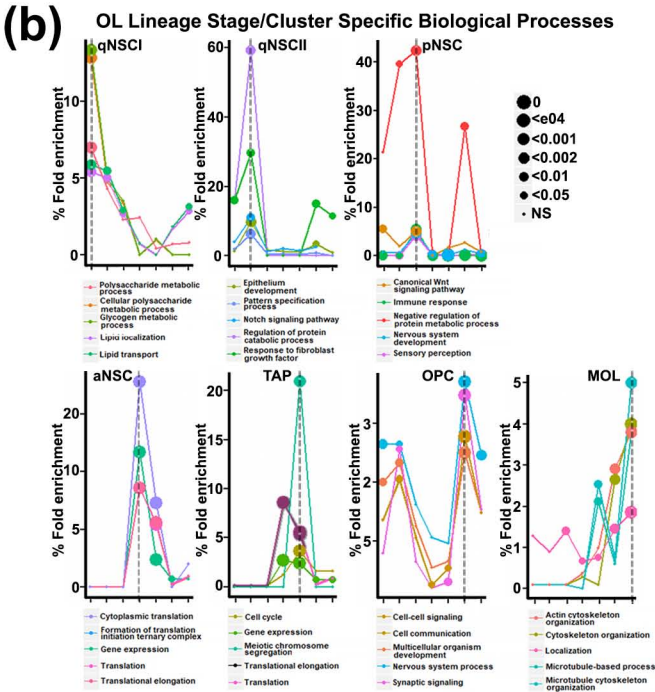
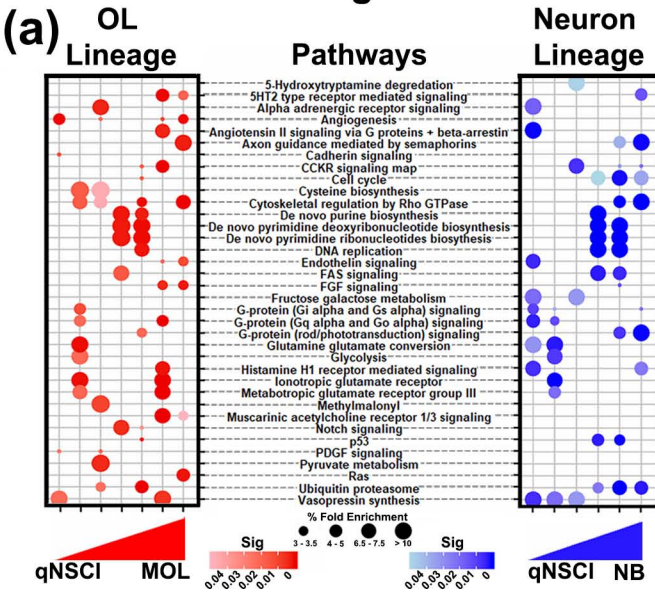


Figure 3: Cell cycle heterogeneity of oligodendroglial and neuronal lineage cells.

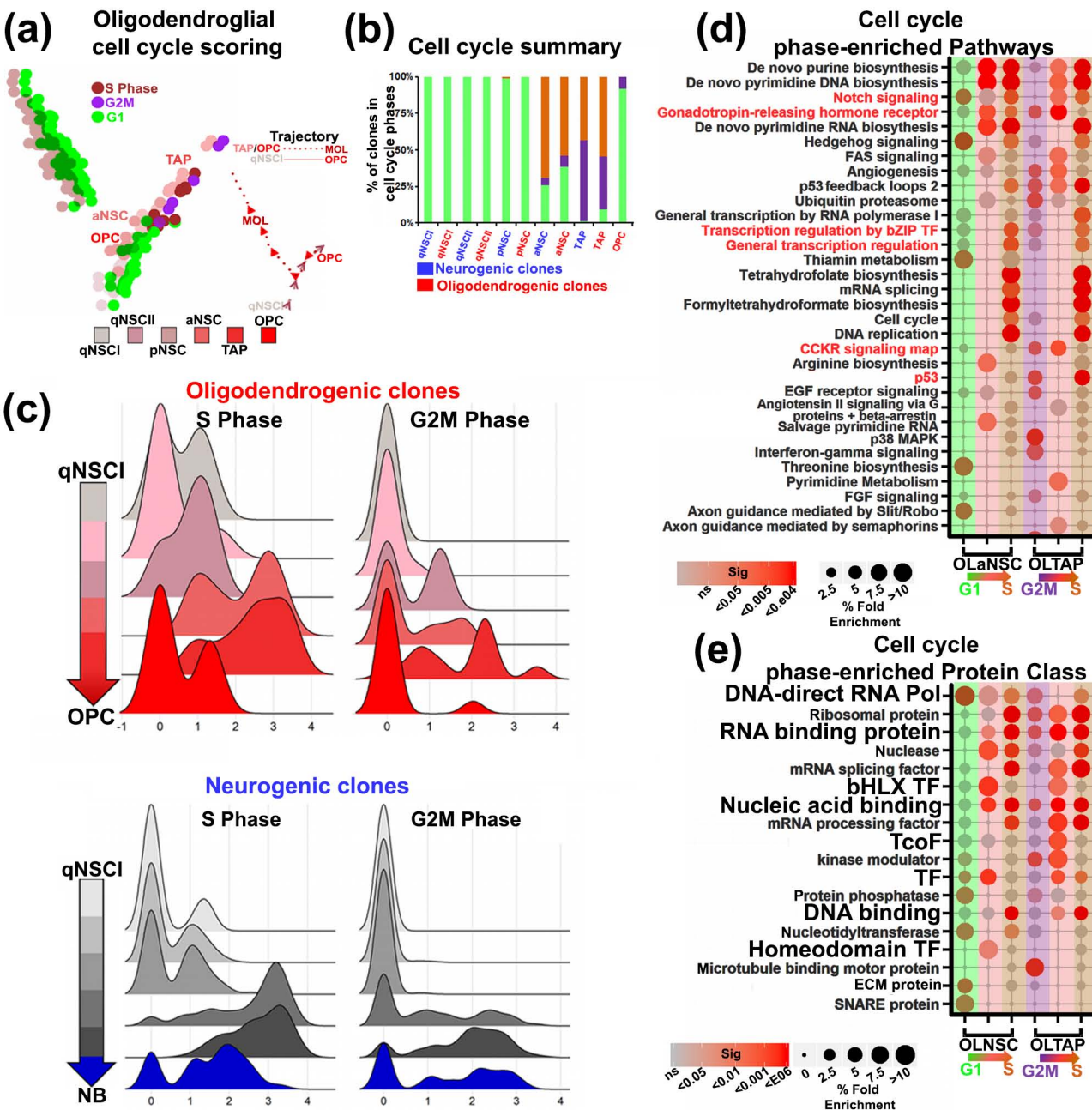


Figure 4: Reconstruction of a GRN by merging of previously generated networks and organization of stages in the oligodendrocyte lineage according to their pseudotime coordinates.

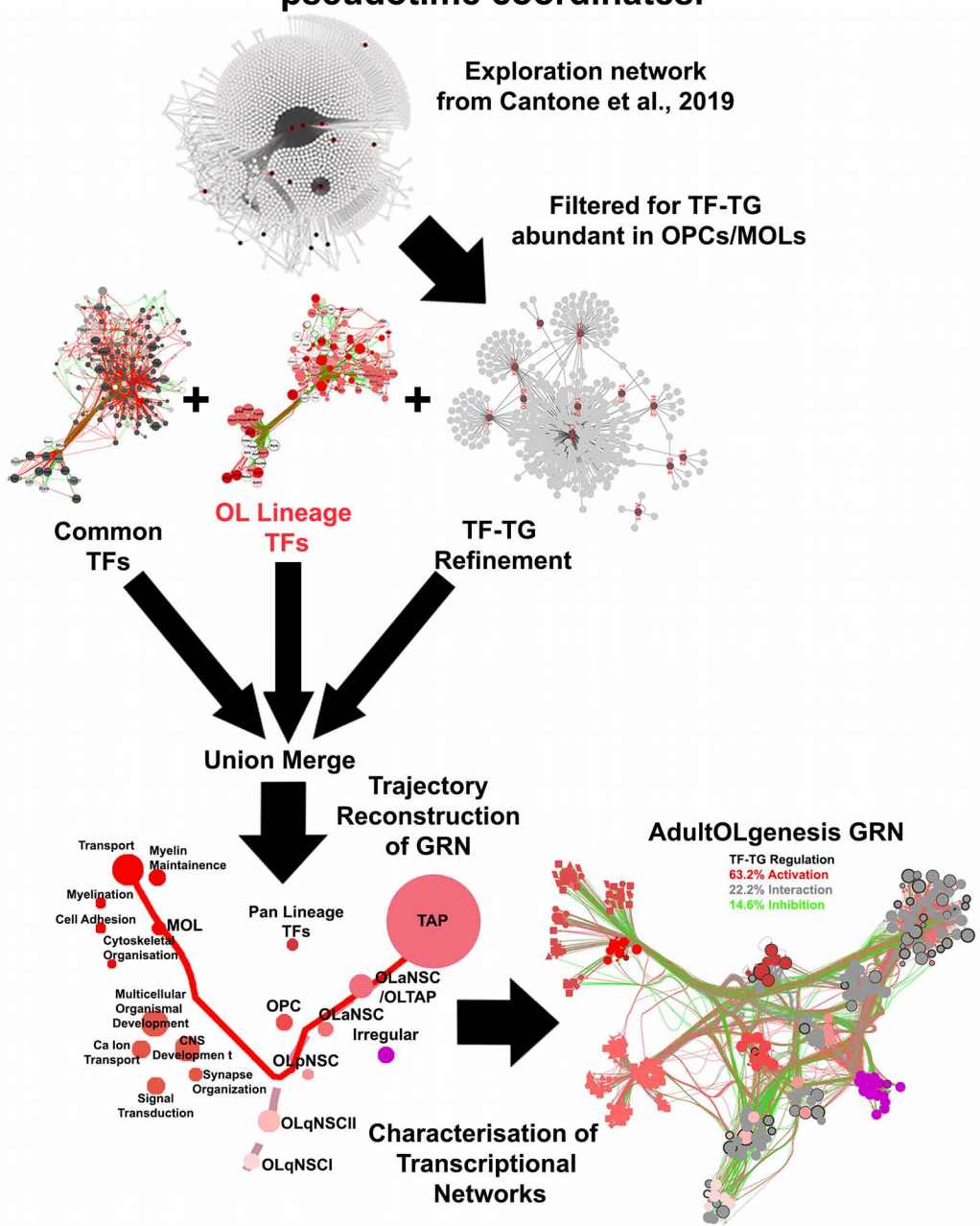


Figure 5: Gene regulatory interactions in substages of the oligodendrocyte lineage and the predicted effects of key transcription factors in each stage.

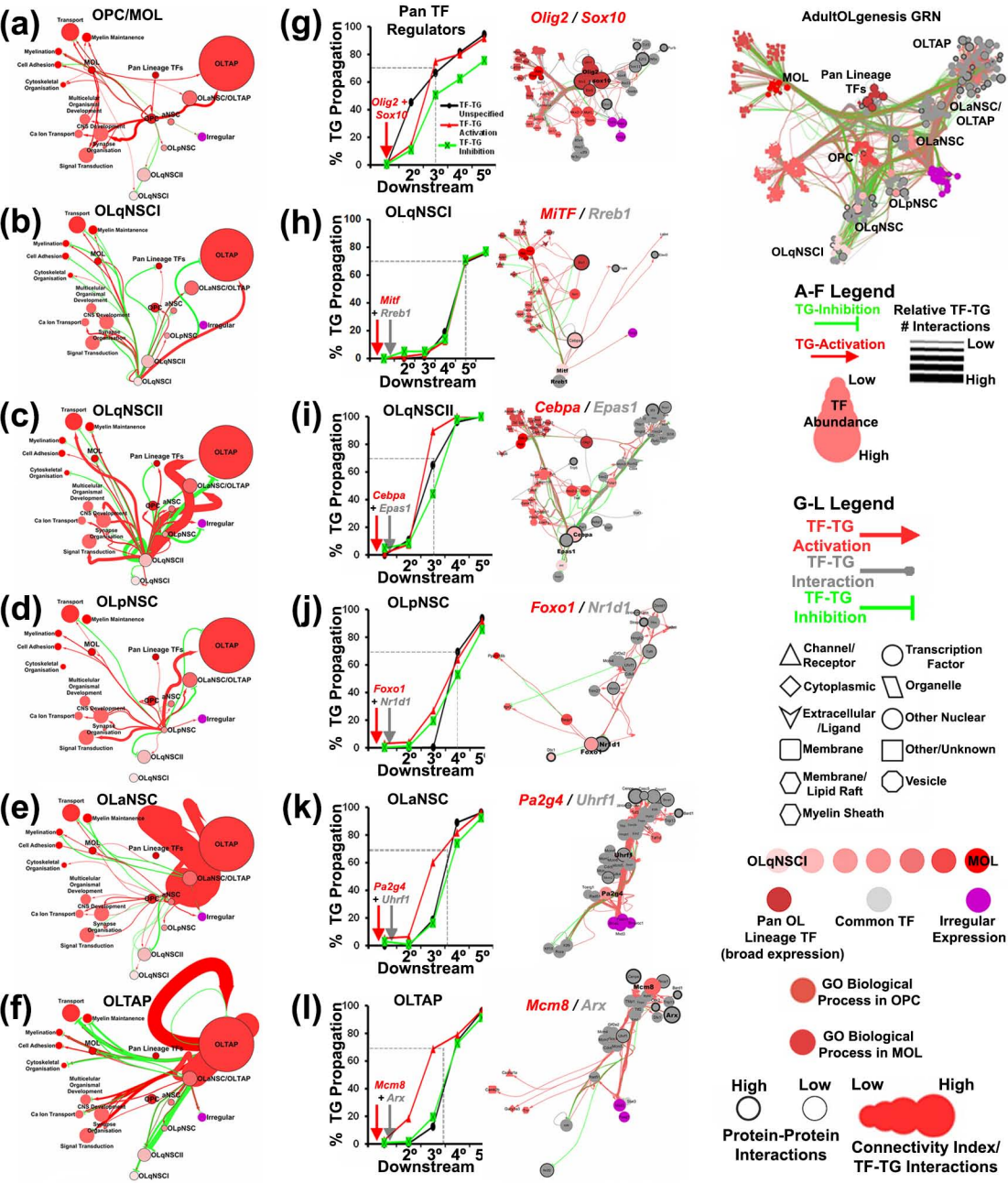
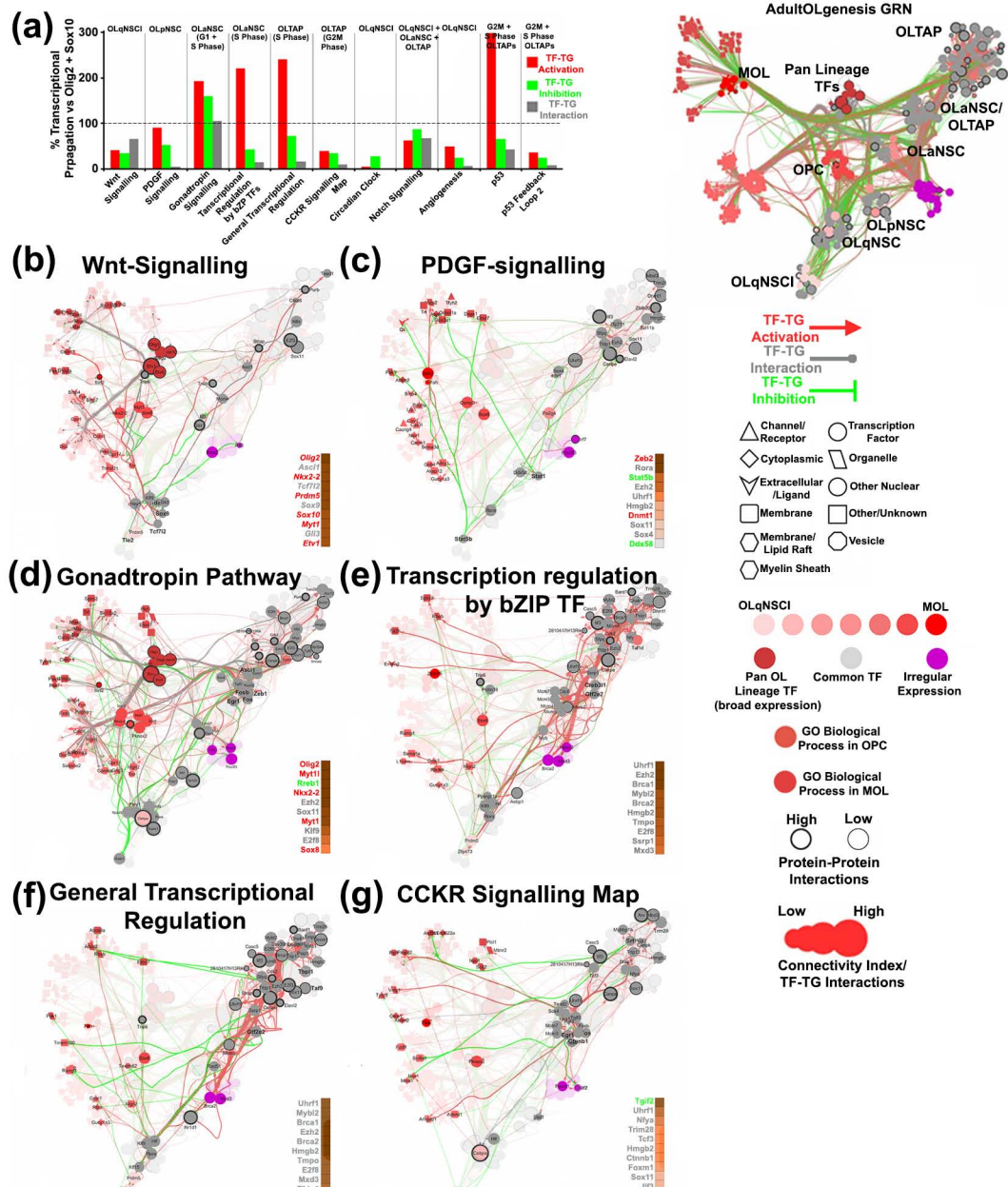


Figure 6: Mapping the impact of Signaling/PANTHER pathways onto GRNs.



Supporting Information

Figure S1:

Summary of the datasets processed and overview of the transcription factor expression comparisons with postnatal bulk and adult single analysis. (a) Datasets re-processed illustrating the transgenic reporter and immunofluorescence strategy for isolating cells derived from the adult SVZ. Processed cells are shown as a tSNE plot. (b) Heatmap demonstrating that transcription factors expressed in single cells of OLqNSCI, OLqNSCII and OLpNSC (single cell early stage oligodendrocytes) group closely with postnatal dorsal bulk datasets. Lists of differentially expressed transcription factor-encoding genes from the indicated analyses were rendered as lists of binary values to allow grouping. (c) Clustergram illustrating transcriptomic differences and similarities of datasets generated from bulk versus single cell sequencing. Abbreviations: aNSC: activated neural stem cell; dTAPs: dorsal TAPs; dSVZ: dorsal subventricular zone; N: neuronal; NB: neuroblast; NSC: neural stem cell; oligodendrocyte: oligodendrocyte; OL: oligodendroglial; OPC: oligodendrocyte precursor cell; PANTHER: protein annotation through evolutionary relationship; PCA: principal component analysis; qNSC: quiescent neural stem cells; TAP: transiently amplifying progenitor.

Figure S2:

Stage and cell specific marker expression across single cells in tSNE plots. (a) Constant *Gapdh* expression levels across cell types studied. (b-g) Selected markers of stage-specific markers, including pan-early NSC populations (*Hes5* qNSC-pNSC) and neuroblasts (*Dcx*). (i-l) Landmark markers of oligodendrocytes. Abbreviations: mOL: mature oligodendrocyte; NSC: neural stem cell; OPC: oligodendrocyte precursor cell; pNSC: primed neural stem cell; qNSCI: quiescent neural stem cell (subtype I); qNSCII: quiescent neural stem cell (subtype II); TAP: transiently amplifying progenitor.

Figure S3:

Stage-specific comparisons of oligodendrocyte lineage versus neuronal lineage for PANTHER Protein Class and Pathways. (a-e) Cluster enriched genes for the oligodendroglial (red throughout) and neuronal lineage (blue throughout) for each stages analysed were compared for Panther Protein Class and Pathways. The overlapping genes (grey throughout) in each stage were included in the analysis. Ontology terms enriched in the oligodendrocyte lineage, neuronal lineage and common to both lineages are highlighted in red, blue and black text, respectively. Abbreviations: NSC: neural stem cell; pNSC: primed neural stem cell; qNSCI: quiescent neural stem cell (subtype I); qNSCII: quiescent neural stem cell (subtype II); TAP: transiently amplifying progenitor; TF: transcription factor.

Figure S4:

Temporal PANTHER Pathway enrichment in the oligodendrocyte lineage. A time course of selected pathways enriched in the oligodendrocyte lineage from the PANTHER analysis shows enrichment of mechanisms during the course of oligodendrogenesis. Red, grey and blue colours in Venn diagrams signify, oligodendroglial, intersect (common), and neuronal lineage cells, respectively. A few pathways such as Angiogenesis and Notch signalling for example show enrichment in defined stages. Terms have been shorted/abbreviated to fit.

Figure S5:

Temporal Transcriptional Regulation in the oligodendrocyte lineage. Protein class terms abundant in the 3 stages in Figure S4 are expanded further as a heatmap for representing modes of transcription factors regulating the oligodendrocyte lineage. TF: transcription factor.

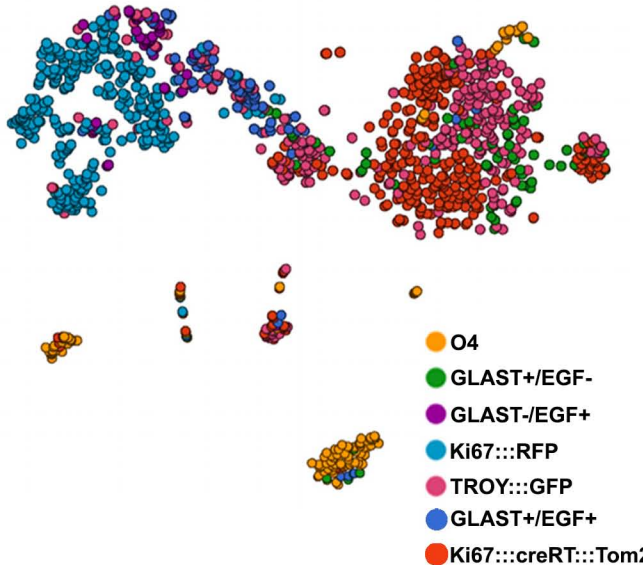
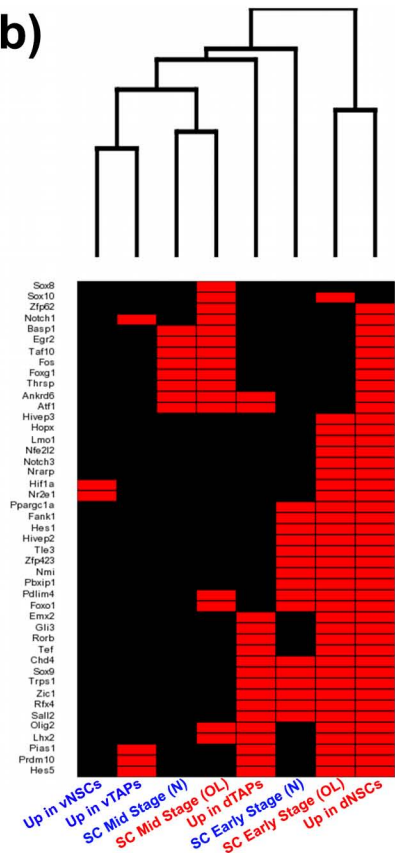
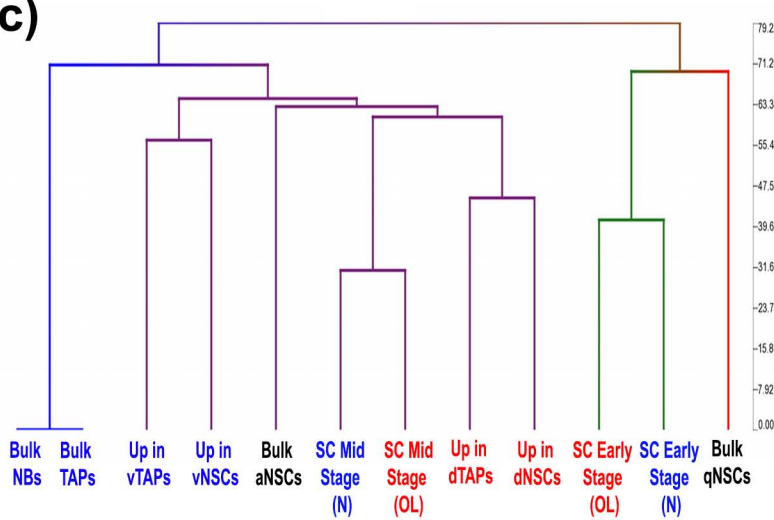
Figure S6:

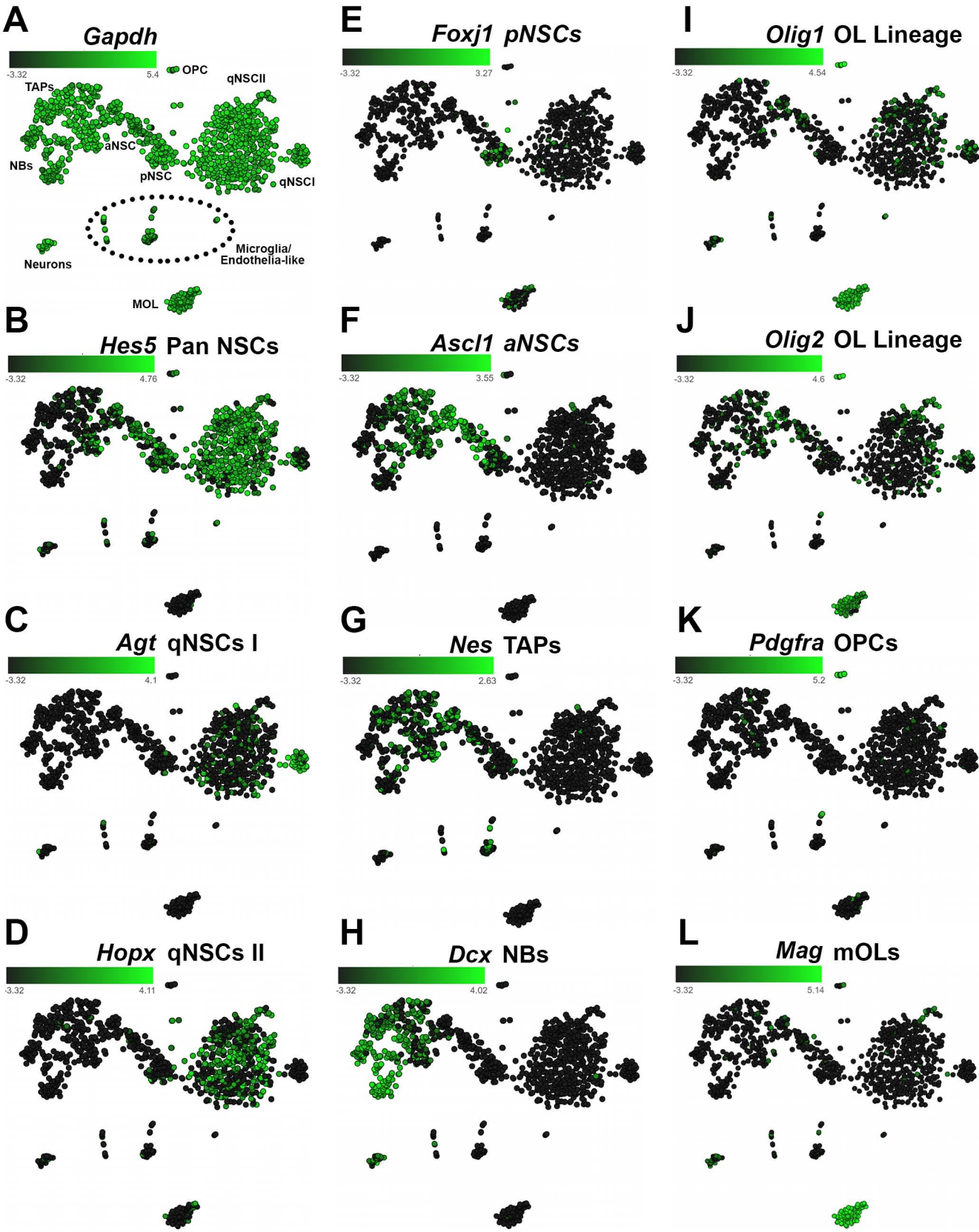
Transcription factor expression in oligodendroglia points to shifts in gene regulatory network states as major drivers of differentiation. (a) Transcription factors expressed in the oligodendrocyte lineage (light red from OLqNSCI to dark red for mature oligodendrocytes) and expressed in both lineages, i.e. commonly expressed transcription factors between the 2 lineages (light grey from qNSCI to dark grey for TAPs) are ranked according to their heat diffusion impact for downstream genetic interactions, physical interactions with other transcription factors and combined. (b-d) Using gene lists for the defined stages for transcription factor expression, those transcription factors expressed in both lineages from qNSCI to TAP stage (b), enriched in the neuronal lineage from qNSCI to the NB stage e and oligodendroglial lineage from OLqNSCI to OPC stage (d). The size of each transcription factor node in the network is relative to its transcription factor-TG (target gene) connectivity index. The numbers of activating (red) or inhibiting (green) interactions from each network are shown as a percentage. (e) The top 25 transcription factors with the highest connectivity index are displayed as heatmaps for the numbers of regulatory interactions with TGs. Heatmaps show darker to lighter colour relative to the numbers of genes regulated by each transcription factor. (f) Examples of higher-, medium- and low-ranking transcription factors. See Figure 4d for description of the legend. Abbreviations: MOL: mature oligodendrocyte; NB: neuroblast; NSC: neural stem cell; OL: oligodendrocyte; OLaNSC: oligodendroglial activated neural stem cell; OLpNSC: oligodendroglial primed neural stem cell; OLqNSCI: oligodendroglial quiescent neural stem cell (subtype I); OLqNSCII: oligodendroglial quiescent neural stem cell (subtype II); OLTAP: oligodendroglial transiently amplifying progenitor; OPC: oligodendrocyte precursor cell; pNSC: primed neural stem cell; qNSCI: quiescent neural stem cell (subtype I); TAP: transiently amplifying progenitor; transcription factor; TG: target gene.

Figure S7:

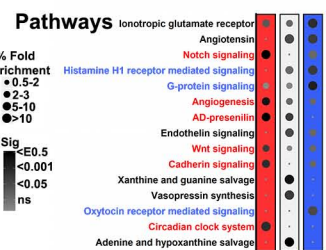
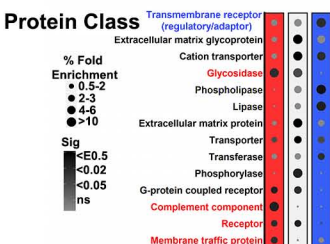
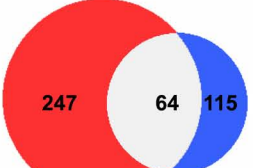
Diffusion ranking for transcription factor functional relationships. (a) Transcription factors expressed in the oligodendrocyte lineage from OLqNSC to MOL stage and those that are common to both oligodendroglial and neuronal lineages were first converted to human gene symbols for maximising the data gathered (information on human gene orthologs are more numerous). (b,c) GeneMania was used to gather functional information on genetic and physical interactions (protein-protein interactions) for the genes sampled. All genes were initially assembled on a network without prior arrangement and the heat diffusion algorithm applied separately for genetic and physical interactions. Node sizes in the networks reflect diffusion rankings for the two combined parameters. Network organized using the CoSE algorithm for force directing nodes within the defined stages. (d) Grading of transcription factors within each stage. Larger to smaller node sizes are relative to the diffusion ranking scores of combined genetic and physical diffusion. Border thickness of each transcription factor directly proportional to protein-protein

interaction number. Transcription factors labels are shown for those prioritised and additional transcription factors shown are expressed in the oligodendrocyte lineage with significant expression, whilst the remaining are derived from more stringent criteria. Abbreviations: MOL: mature oligodendrocyte; NSC: neural stem cell; OL: oligodendrocyte; OLaNSC: oligodendroglial activated neural stem cell; OLpNSC: oligodendroglial primed neural stem cell; OLqNSC_I: oligodendroglial quiescent neural stem cell (subtype I); OLqNSC_{II}: oligodendroglial quiescent neural stem cell (subtype II); OLTAP: oligodendroglial transiently amplifying progenitor; OPC: oligodendrocyte precursor cell; pNSC: primed neural stem cell; qNSC_I: quiescent neural stem cell (subtype I); TAP: transiently amplifying progenitor; transcription factor.

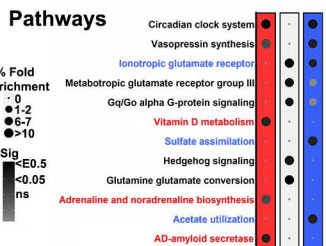
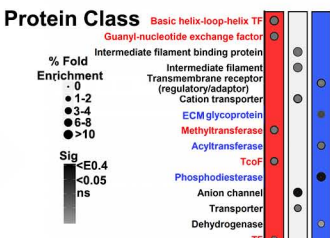
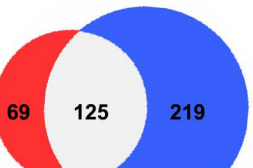
(a)**(b)****(c)**



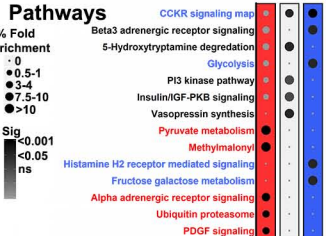
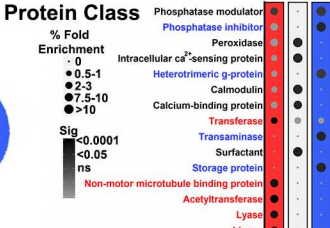
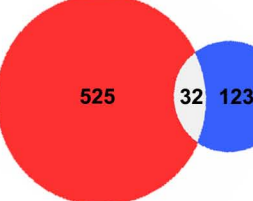
(a) qNSCI



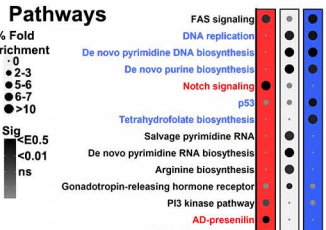
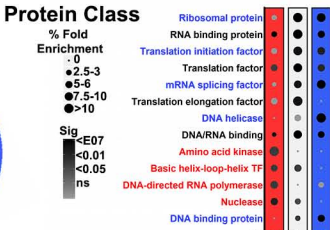
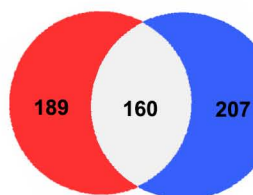
(b) qNSCII



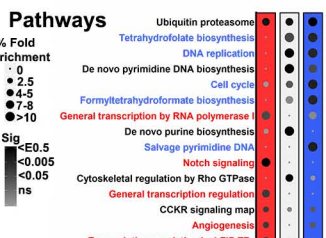
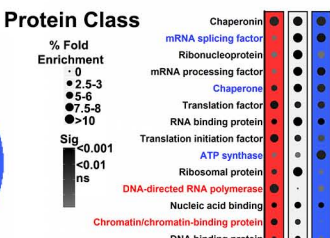
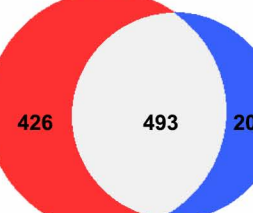
(c) pNSC

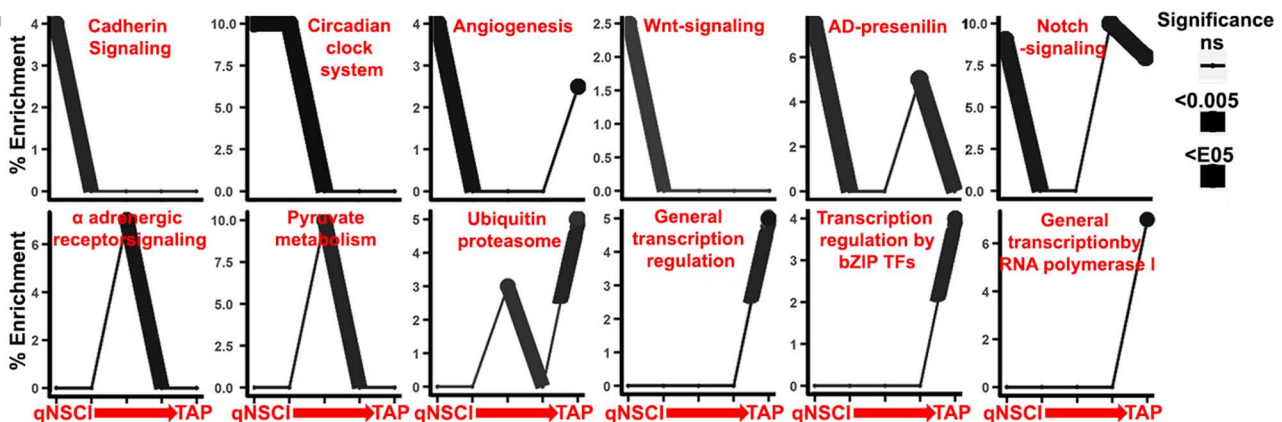


(d) aNSC



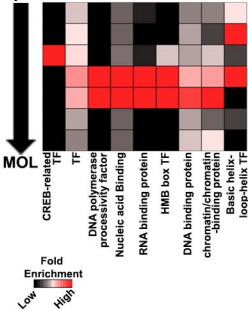
(e) TAP

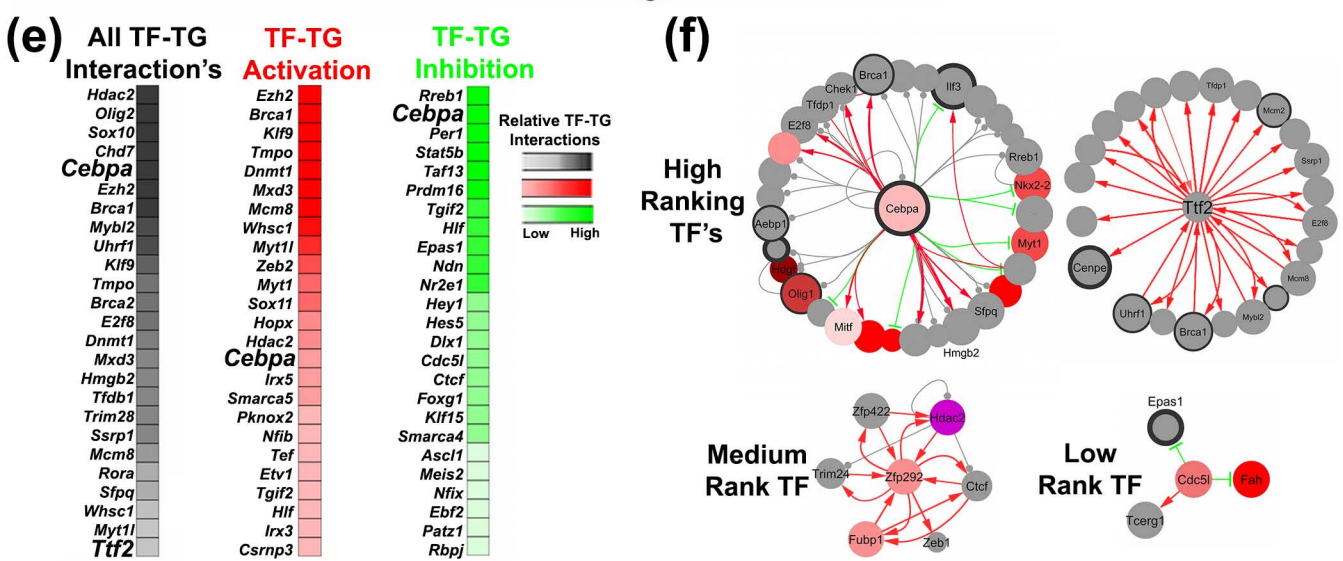
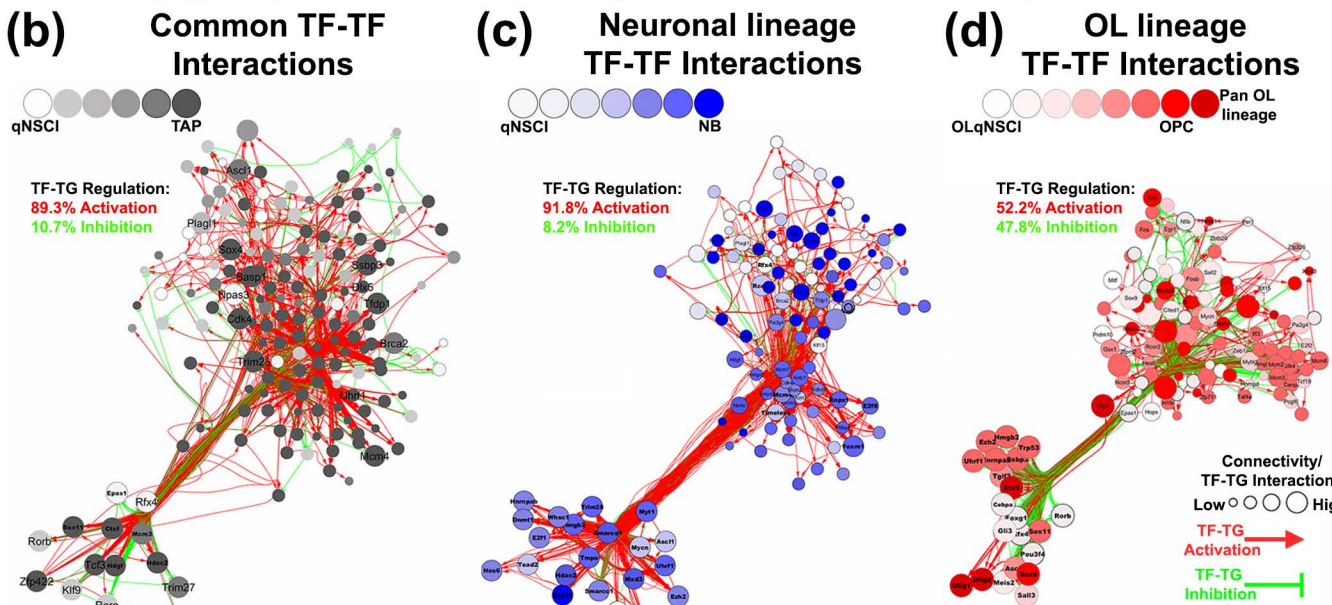
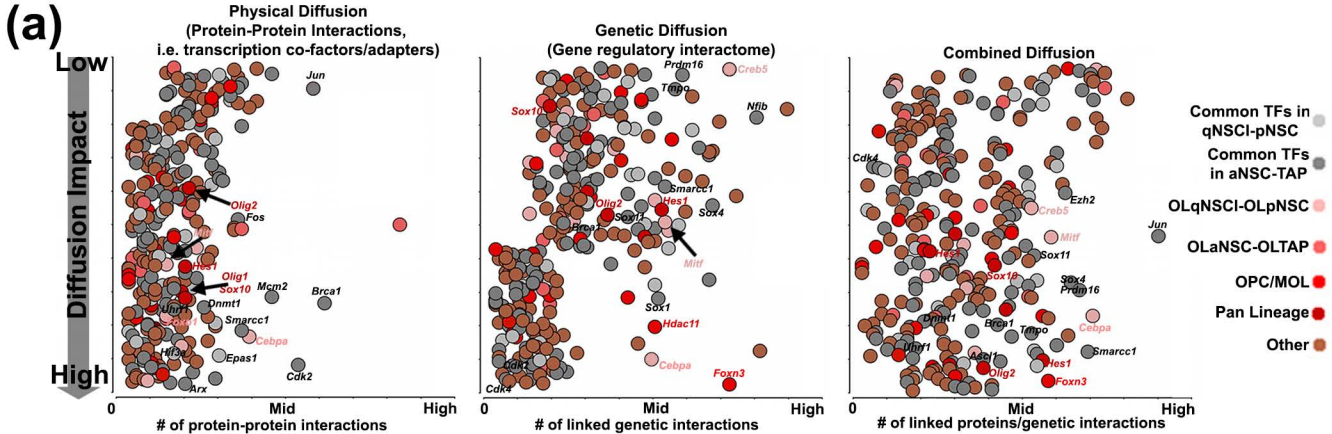


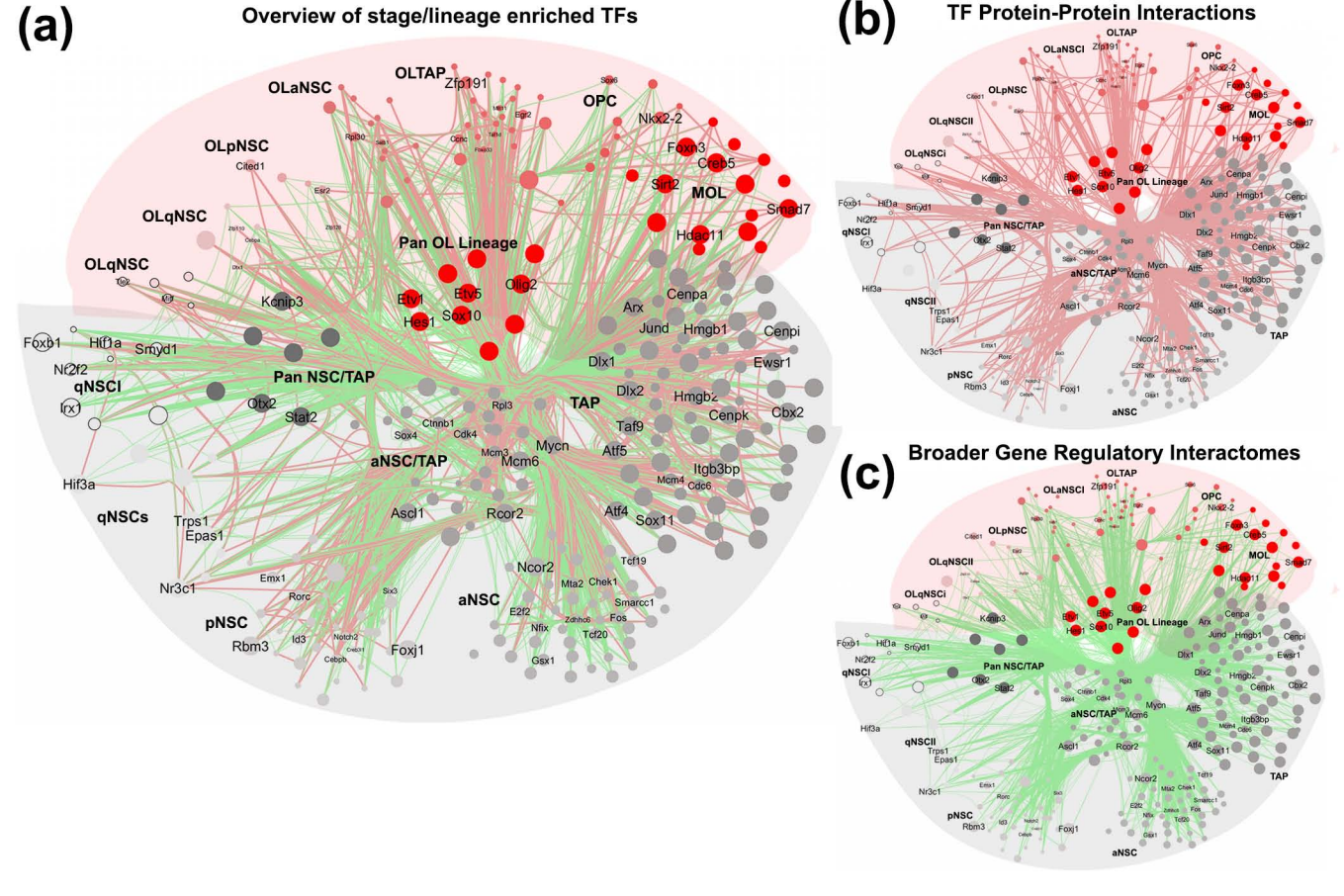


Expanded TF Protein Class

OLqNSCI







(d) TF Ranking for Genetic and Protein-Protein Interactions

Oligodendrogenesis/Lineage Progression

